



U.S. DEPARTMENT OF
ENERGY

PNNL-19524

Prepared for the U.S. Department of Energy
under Contract DE-AC05-76RL01830

Hanford 100-N Area In Situ Apatite and Phosphate Emplacement by Groundwater and Jet Injection: Geochemical and Physical Core Analysis

JE Szecsody
VR Vermeul
JS Fruchter
MD Williams
ML Rockhold
NP Qafoku
JL Phillips

July 2010



Pacific Northwest
NATIONAL LABORATORY

*Proudly Operated by **Battelle** Since 1965*

DISCLAIMER

This report was prepared as an account of work sponsored by an agency of the United States Government. Neither the United States Government nor any agency thereof, nor Battelle Memorial Institute, nor any of their employees, makes **any warranty, express or implied, or assumes any legal liability or responsibility for the accuracy, completeness, or usefulness of any information, apparatus, product, or process disclosed, or represents that its use would not infringe privately owned rights**. Reference herein to any specific commercial product, process, or service by trade name, trademark, manufacturer, or otherwise does not necessarily constitute or imply its endorsement, recommendation, or favoring by the United States Government or any agency thereof, or Battelle Memorial Institute. The views and opinions of authors expressed herein do not necessarily state or reflect those of the United States Government or any agency thereof.

PACIFIC NORTHWEST NATIONAL LABORATORY
operated by
BATTELLE
for the
UNITED STATES DEPARTMENT OF ENERGY
under Contract DE-AC05-76RL01830

Printed in the United States of America

**Available to DOE and DOE contractors from the
Office of Scientific and Technical Information,
P.O. Box 62, Oak Ridge, TN 37831-0062;
ph: (865) 576-8401
fax: (865) 576-5728
email: reports@adonis.osti.gov**

**Available to the public from the National Technical Information Service,
U.S. Department of Commerce, 5285 Port Royal Rd., Springfield, VA 22161
ph: (800) 553-6847
fax: (703) 605-6900
email: orders@ntis.fedworld.gov
online ordering: <http://www.ntis.gov/ordering.htm>**



This document was printed on recycled paper.

(9/2003)

Hanford 100-N Area In Situ Apatite and Phosphate Emplacement by Groundwater and Jet Injection: Geochemical and Physical Core Analysis

JE Szecsody
VR Vermeul
JS Fruchter
MD Williams
ML Rockhold
NP Qafoku
JL Phillips

July 2010

Prepared for
CH2M HILL Plateau Remediation Company
under Contract DE-AC05-76RL01830

Pacific Northwest National Laboratory
Richland, Washington 99352

Abstract

The purpose of this study is to evaluate emplacement of phosphate into subsurface sediments in the Hanford Site 100-N Area by two different technologies: groundwater injection of a Ca-citrate-PO₄ solution and water-jet injection of sodium phosphate and/or fish-bone apatite. Because groundwater injections of Ca-citrate-PO₄ into the upper portion of the Hanford formation requires injections at high river stage, alternate strategies such as Ca-citrate-PO₄ solution infiltration and jet injection of phosphate mass are also being investigated. In situ emplacement of phosphate and apatite results in initial adsorption, followed by incorporation of Sr-90 into the apatite structure by isomorphic substitution for calcium. Sufficient apatite (1.7 mg apatite/g or 0.54 mg PO₄/g sediment, occupies 14% of the pore space) needs to be emplaced uniformly in both the Hanford formation and Ringold Formation to prevent groundwater migration of Sr-90 into the Columbia River. Sediment cores collected 1 year after high-concentration Ca-citrate-PO₄ groundwater injections showed the Hanford formation received an average of 0.56 ± 0.25 mg PO₄/g and the Ringold Formation received an average of 0.27 ± 0.11 mg PO₄/g. Phosphate precipitation was relatively uniform with distance from the injection well (core samples at radial distance of 6.5, 10, and 15.7 ft), likely because the use of the Ca-citrate-PO₄ solution allows tens of hours of injection before precipitation occurs. Core analysis also showed that low aqueous Sr-90 values observed in the field are caused by incorporation of Sr-90 into apatite (39.4% of the mass by 1 year), and ion exchange flushing due to the Ca-citrate-PO₄ solution injection (47% of the mass). Sediments that were jet injected with sodium phosphate or fish-bone apatite (or both) showed high phosphate concentrations (0.80 to 2.7 mg/g) with multiple (6), closely spaced (~5 ft spacing) injection points. However, with samples taken very close to injection points (1.0, 2.5, and 3.8 ft), it is difficult to assess the relevant areal extent at greater distance (i.e., 5 to 20 ft) and to make recommendations regarding future injection point spacing greater than 5-ft apart. Jet injection of sodium phosphate only averaged 1.2 ± 2.0 mg PO₄/g of sediment (at 1.1 ft), jet injection of fish-bone apatite averaged 1.6 ± 1.4 mg PO₄/g (at 1.0 ft), and jet injection of sodium phosphate and fish-bone apatite averaged 2.7 ± 3.0 mg PO₄/g (at 2.5 ft) and 0.8 ± 0.5 mg PO₄/g (at 3.8 ft). High phosphate mass can lead to a decrease in permeability, although it is unclear how much pore space the precipitate is occupying for jet injections as the system is likely physically altered by liquifaction (fine grained sediments) or fractures. In addition, jet injection appears to deposit more phosphate in finer grained sediments, so the spatial variability of the phosphate mass is much greater (standard deviation was 81% of the mean phosphate mass) than Ca-citrate-PO₄ injections (standard deviation was 43% of the mean). A mechanism that could explain these results is that finer-grained sediments are involved in liquifaction during jet injections, which could result in more complete mixing of the phosphate in the sediment, whereas dendritic fracture patterns may develop with jet injection into coarser grained sediments. This may also cause some change in the sediment hydraulic conductivity. Overall, both technologies (groundwater injection of Ca-citrate-PO₄) and water-jet injection of sodium phosphate/fish-bone apatite) delivered sufficient phosphate to subsurface sediments in the 100-N Area to affect Sr-90 adsorption and precipitation. Over years to decades, additional Sr-90 will be incorporated into the apatite precipitate from all phosphate sources. Therefore, high pressure water jetting does appear to be a viable technology for emplacing phosphate or apatite in shallow subsurface sediments (using closely spaced injection points) that are difficult to access by Ca-citrate-PO₄ groundwater injections. Further analyses are needed to quantify the relevant areal extent of phosphate deposition (in the 5- to 20-ft distance from injection points) and the cause of the high deposition in finer-grained sediments.

Contents

Abstract.....	iii
1.0 Introduction	1.1
2.0 Background: Location of Boreholes.....	2.1
3.0 Experimental Methods.....	3.1
3.1 Geochemical Analysis of Cores	3.1
3.2 Physical Analysis of Cores: Grain-Size Distribution, K_{sat}	3.3
4.0 Results for Groundwater Injection Area.....	4.1
4.1 Phosphate Mass in Cores.....	4.1
4.2 Sr-90 Distribution in Cores	4.6
4.3 Ion Exchangeable Calcium and Strontium	4.7
4.4 Grain-Size Distribution and Hydraulic Conductivity.....	4.7
4.5 River Sediment Sample Analysis.....	4.9
5.0 Results in Jet Core Injection Area	5.1
5.1 Phosphate Mass in Cores.....	5.1
5.2 Sr-90 Distribution in Cores	5.6
5.3 Ion Exchangeable Calcium and Strontium.....	5.7
5.4 Grain-Size Distribution and Hydraulic Conductivity.....	5.7
5.5 Fish-Bone Organic Matter and Influence on Sr-90 Mobility	5.7
6.0 Summary.....	6.1
6.1 Phosphate and Sr-90 Distribution in River Sediments	6.1
6.2 Groundwater Injection of Ca-Citrate- PO_4	6.1
6.3 Jet-Injected Phosphate and Apatite	6.2
6.4 Comparison of Groundwater and Jet Injections	6.4
7.0 References	7.1
Appendix A – Jet-Injection Grain-Size Distributions.....	A.1
Appendix B – Well-Injection Grain-Size Distributions.....	B.1

Figures

2.1	Injection Well Location in the Hanford Site 100-N Area	2.1
2.2	Monitoring Wells and Boreholes near N-137	2.1
2.3	Location of Jet Injections and Boreholes.....	2.3
2.4	Location of River Sediment Samples	2.4
3.1	Phosphate Extraction from Sediment by Acid Dissolution	3.1
3.2	Phosphate Extraction from Sediment by Acid Dissolution for Different Grain-Size Distributions.....	3.2
3.3	Mineral Phase Identification of a Location with High Phosphorous Concentration; Electron Backscatter of the Location is Indicative of a Surface Precipitate, with Identification of this Mineral as Apatite by Comparison to an Apatite Standard	3.3
4.1	Scanning Electron Microscope Pictures of Sediment with Identification of Minerals by EDS Detector	4.1
4.2	N-368 Vertical Profiles of Sr-90, PO ₄ , Ion Exchangeable Strontium, Ion Exchangeable Calcium, Calculated Saturated Hydraulic Conductivity, and Fraction Grain Size less than 4 mm	4.2
4.3	N-369 Vertical Profiles of Sr-90, PO ₄ , Ion Exchangeable Strontium, Ion Exchangeable Calcium, Calculated Saturated Hydraulic Conductivity, and Fraction Grain Size less than 4 mm	4.3
4.4	N-370 Vertical Profiles of Sr-90, PO ₄ , Ion Exchangeable Strontium, Ion Exchangeable Calcium, Calculated Saturated Hydraulic Conductivity, and Fraction Grain Size less than 4 mm	4.4
4.5	Correlation Between Saturated Hydraulic Conductivity and Total Sr-90 and PO ₄ in Sediment	4.8
4.6	Correlation of Total Sr-90 and Phosphate in Sediment Cores	4.8
5.1	N-222 Vertical Profiles of Sr-90, PO ₄ , Ion Exchangeable Strontium, Ion Exchangeable Calcium, Calculated Saturated Hydraulic Conductivity, and Fraction Grain Size less than 4 mm	5.2
5.2	N-220 Vertical Profiles of Sr-90, PO ₄ , Ion Exchangeable Strontium, Ion Exchangeable Calcium, Calculated Saturated Hydraulic Conductivity, and Fraction Grain Size less than 4 mm	5.3
5.3	N-219 Vertical Profiles of Sr-90, PO ₄ , Ion Exchangeable Strontium, Ion Exchangeable Calcium, Calculated Saturated Hydraulic Conductivity, and Fraction Grain Size less than 4 mm	5.4
5.4	N-217 Vertical Profiles of Sr-90, PO ₄ , Ion Exchangeable Strontium, Ion Exchangeable Calcium, Calculated Saturated Hydraulic Conductivity, and Fraction Grain Size less than 4 mm	5.5
5.5	Correlation Between Grain Size and PO ₄ and Saturated Hydraulic Conductivity and PO ₄	5.6
5.6	Calculated Saturated Hydraulic Conductivity Values for Jet-Injected Cores	5.8
5.7	Organic Carbon and Inorganic Carbon Depth Profile	5.9
6.1	Phosphate Content and Distance from Injection.....	6.5

Tables

2.1	Surveyed Location of Groundwater Injection Boreholes	2.1
2.2	Surveyed Location of Jet-Injection Boreholes and Distance to Jet Injections.....	2.2
2.3	Surveyed Location of River Sediment Samples	2.4
4.1	Average Phosphate Concentration in Groundwater Injected Boreholes.....	4.5
4.2	Calculated Sr-90 Adsorption to Sediment in Apatite in Mixed Systems.....	4.7
4.3	River Sediment Analysis	4.9
5.1	Phosphate Content in Water-Jet Injected Boreholes.....	5.6
5.2	Carbon Analysis of River Samples	5.9
5.3	Ultraviolet Light Treatment and Sr-90 Release	5.10
6.1	Phosphate Content in All Boreholes	6.5

1.0 Introduction

The purpose of this study is to evaluate emplacement of phosphate into subsurface sediments in the Hanford Site 100-N Area by two different technologies: water-jet injection of sodium phosphate and groundwater injection of a calcium-citrate-phosphate solution. In situ emplacement of phosphate leads to adsorption and apatite precipitation, and incorporation of Sr-90 into the apatite structure by substitution for calcium (LeGeros et al. 1979; Moore et al. 2004). To prevent groundwater migration of Sr-90 in the 100-N Area from discharging to the Columbia River, sufficient apatite needs to be emplaced uniformly in both the Hanford formation and Ringold Formation (Szecsody et al. 2007, 2009). For the groundwater injection of Ca-citrate-PO₄, cores from three boreholes (N-368, N-369, N-370) drilled at different distances from an injection well (N-137) were characterized. For the jet-injection site, cores from four boreholes were characterized that included N-217 (sodium phosphate jet-injection area), N-222 (solid fish-bone apatite or “Apatite II” [Wright et al. 2004] jet-injection area), and N-219/N-220 (both sodium phosphate and fish-bone apatite jet-injection area). An additional objective of sampling from sites where groundwater injection of a Ca-citrate-PO₄ solution was performed was to characterize the form of the in situ precipitated phosphate (by electron microprobe techniques).

The goal of the injections was to achieve a relatively uniform (aerial and with depth) phosphate distribution in subsurface sediments, with an average target concentration of 1.7 mg apatite/g of sediment (0.54 mg PO₄/g of sediment). Phosphate analysis was conducted on sediment cores. The Sr-90 mass distribution on sediment was characterized by analysis of a) total Sr-90, b) ion exchangeable Sr-90, and c) ion exchangeable strontium and calcium. To understand the spatial variability in phosphate emplacement, the sediment was physically characterized by measuring grain-size distributions, which were used to estimate the saturated hydraulic conductivity using empirical relationships. Groundwater injections of a low concentration Ca-citrate-PO₄ (10 mM PO₄) were previously analyzed by core analysis and showed a relatively uniform phosphate distribution in the aquifer in spite of heterogeneities (Williams et al. 2008; Szecsody et al. 2009). Aqueous breakthrough curve data from high-concentration Ca-citrate-PO₄ (40 mM PO₄) also showed relatively uniform phosphate movement (Vermeul et al. 2010). Because the jet-injection technology is relatively new, for the purpose of apatite injection into Hanford sediments, sediment chemical analysis and grain-size characterization was needed to understand trends in phosphate mass. Jet injection into relatively coarse-grained formations is reported to follow dendritic patterns (ARS Consultants, injection of zero valent iron) whereas jet injection into fine-grained formations can liquify the formation, resulting in more complete mixing. Therefore, finer-grained zones at higher water content may be easier to inject into via jetting, and result in a higher phosphate concentration (with less areal extent) if the jet-injection process is uniform with depth. Sr-90 characterization was conducted in order to a) identify the Sr-90 in the sediment at an aerial location previously uncharacterized, b) obtain the depth distribution, and c) determine how much Sr-90 incorporation into apatite has occurred. Ion exchangeable calcium and strontium are used to characterize how much cation exchange has occurred as a result of the jet injections. The fish-bone apatite that was injected contains 25% to 45% organic matter, so some cores were also analyzed for total organic carbon (TOC).

2.0 Background: Location of Boreholes

Three boreholes were drilled near groundwater injection well N-137 (Figure 2.1) approximately 1 year after high concentration Ca-citrate-PO₄ injection (40 mM PO₄) to characterize the phosphate and Sr-90 distribution in subsurface sediments. These boreholes were located 6.5 ft from the injection (borehole N-368), 10.0 ft from the injection well (borehole N-369), and 15.7 ft from the injection well (borehole N-370), as shown in Figure 2.2 (coordinates in Table 2.1). Aqueous analysis of phosphate from these samples associated with injection of Ca-citrate-PO₄ solution into N-137 (and nearby N-159) indicated that phosphate was distributed over the full distance between the injection and sampling points in both the Ringold Formation and Hanford formation. Phosphate concentration is expected to decrease with distance from the injection well, although N-370 (borehole at 15.7 ft from N-137, 9.5 ft from Ringold only injection well N-159) also received phosphate from the adjacent injection well N-159.

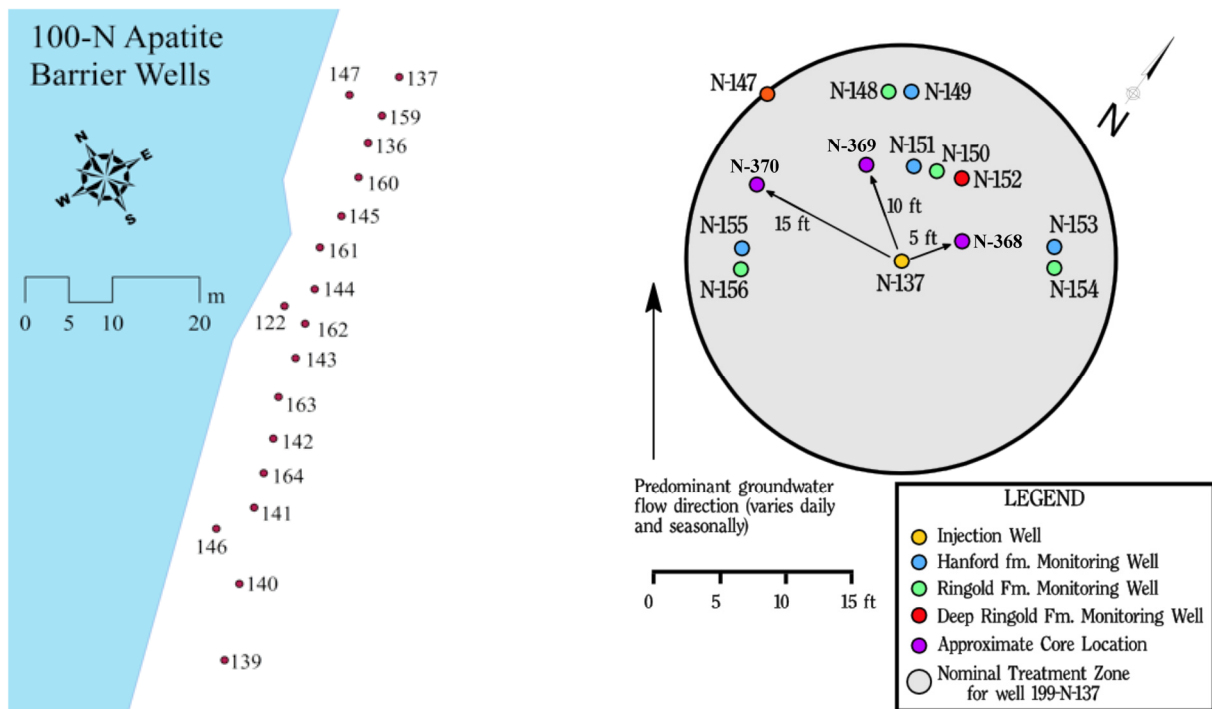


Figure 2.1. Injection Well Location in the Hanford Site 100-N Area

Figure 2.2. Monitoring Wells and Boreholes near N-137

Table 2.1. Surveyed Location of Groundwater Injection Boreholes

Well #	boring	Easting (meters)	Northing (meters)	distance from inj. well N-137	distance from inj. well N-159
199-N-368	C7460	571344.4	149948.3	6.5 ft north	23.0 ft north
199-N-369	C7461	571341.8	149947.7	10.0 ft NW	17.0 ft NW
199-N-370	C7462	571339.7	149945.7	15.7 ft SW	9.5 ft NW

To characterize the amount of phosphate and apatite injected by jet injection, four boreholes were drilled to 22 to 27 ft depth, with continuous sample collection from 6 ft to total depth. The location of this jet-injection area is 200 to 270 ft to the southwest of N-138 (Figure 2.3). The surveyed locations (Table 2.2) show that well 199-N-222 (C7305; fish-bone injection) is 200 ft southwest of N-138. The location of the other boreholes is calculated from N-222. Relative to N-222, well N-220 (C7307; phosphate and fish-bone injection) is 8.5 ft to the southwest, well N-219 (C7308; phosphate and fish-bone injection) is 13 ft to the southwest, and well N-217 (C7310; sodium phosphate injection) is 22 ft to the southwest.

Table 2.2. Surveyed Location of Jet-Injection Boreholes and Distance to Jet Injections

Well #	boring	Easting (meters)	Northing (meters)	distance to (ft)	jet borehole
north grid, fish bone apatite only injection (200 ft SW from N-138)					
199-N-222	C7305	571251.4	149838.5	0.99	C7713
				5.09	C7712
				5.27	C7714
				5.77	C7716
				6.04	C7717
				8.43	C7715
south grid, Na-PO4 only injection					
199-N-217	C7310	571238.8	149820.2	1.06	C7700
				3.74	C7703
				5.18	C7704
				6.37	C7701
				9.13	C7705
				11.38	C7702
center grid, fish bone apatite and Na-PO4 injection					
199-N-219	C7308	571244	149827.8	2.51	C7706
				5.82	C7707
				7.44	C7709
199-N-220	C7307	571246.5	149831.50	3.78	C7711
				4.19	C7708
				7.57	C7710

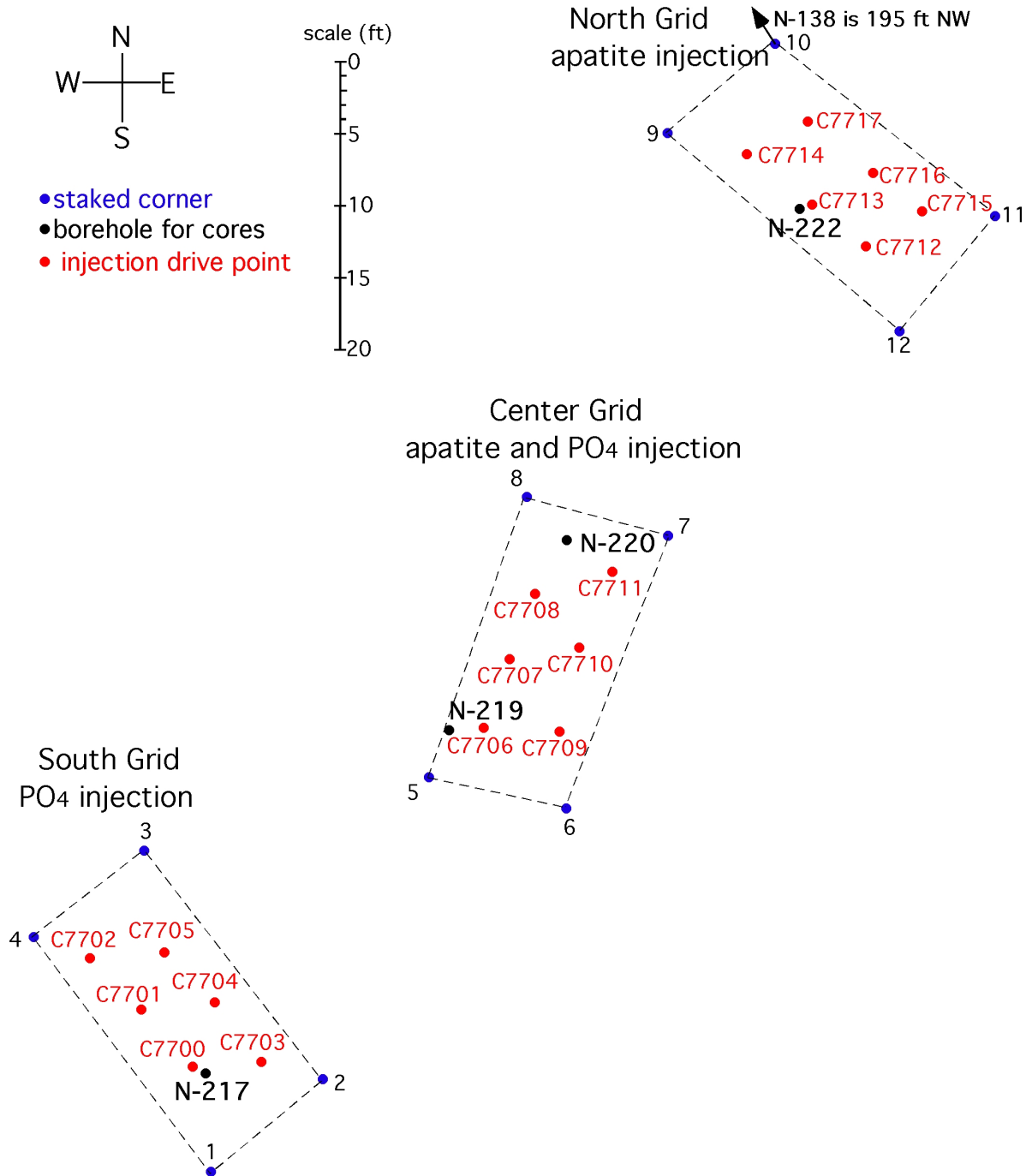


Figure 2.3. Location of Jet Injections and Boreholes

Two river sediment samples were also collected by Heather Sulloway (Washington Closure Hanford, LLC) to measure Sr-90 and phosphate concentrations. The “T100N3a” sample was from river sediment near (i.e., 200 ft northwest) the Ca-citrate-PO₄ groundwater injection well N-138, in the zone of elevated Sr-90 contamination and may also contain some phosphate (Table 2.3, Figure 2.4). River sediment sample “N outfall” was from a location 1320 ft upriver from T100N3a, in an area of lower Sr-90 contamination, and should only contain background phosphate.

Table 2.3. Surveyed Location of River Sediment Samples

river sample	Easting (meters)	Northing (meters)	distance from N-138
N Outfall	571030.9	149577.8	1320 ft SW
T100N3a	571305.9	149945.6	199.5 ft NW

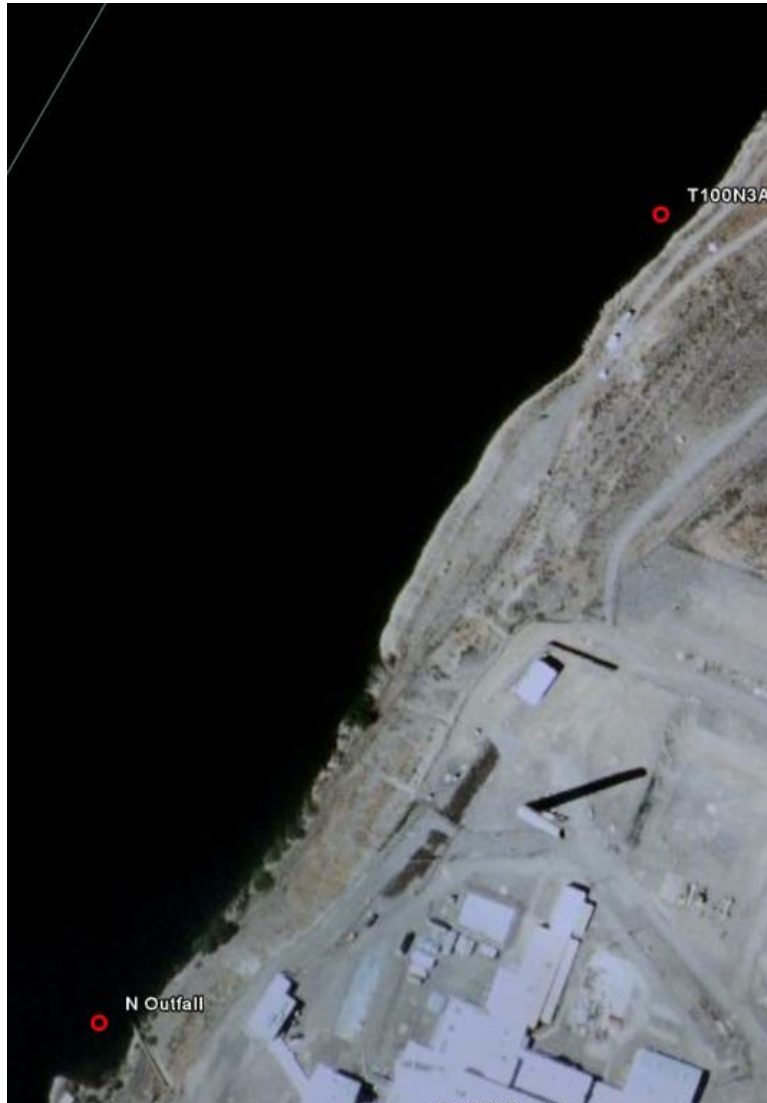


Figure 2.4. Location of River Sediment Samples

3.0 Experimental Methods

3.1 Geochemical Analysis of Cores

Phosphate mass in sediment was measured using an acid dissolution extraction method. Acid dissolution of the sediment/apatite mixture will result in PO_4 from both sediment minerals and the added apatite. Because the added apatite occurs in the form of relatively small (sub micron) crystals, a weak acid treatment for a limited amount of time was used to dissolve all the added apatite but dissolve less of the sediment mineral phase PO_4 . Initial experiments with 0.5 M and 5.0 M HNO_3 (Szecsody et al. 2007, 2009; Chairat et al. 2004) showed that within 15 minutes, aqueous PO_4 had reached equilibrium. For the acid dissolution of the pure apatite (no sediment), the amount recovered was equal to the predicted amount for both the 0.5 M and 5 M HNO_3 cases, indicating that the lower acid concentration was sufficient to remove and quantify apatite formed by the treatment processes. Ultimately both the 0.5 M and 0.1 M HNO_3 treatments for 15 minutes could be used to dissolve the added apatite (Figure 3.1), where the slopes were the same (i.e., because of the same amount of addition). The intercepts (i.e., baseline PO_4 from sediment minerals dissolving) differed with the weaker acid dissolving less of the apatite minerals, as expected, so produced a lower baseline. The background (baseline) phosphate extracted from the sediment (with no added apatite) was 0.45 mg/g. The slope of 0.86 means the method recovered approximately 86% of the apatite added. Subsequent results in this study subtract out the baseline phosphate concentration so that the observed phosphate concentration is the result of the Ca-citrate- PO_4 added.

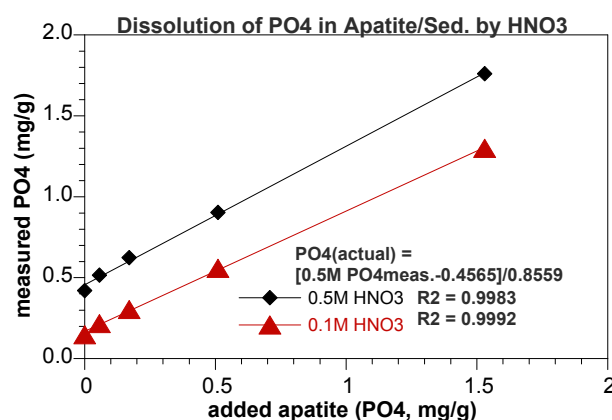


Figure 3.1. Phosphate Extraction from Sediment by Acid Dissolution (calibration curve)

In a prior study, the baseline phosphate for 100-N Area sediments was measured in 11 sediments from wells that were obtained before any Ca-citrate- PO_4 injections (Szecsody et al. 2009). For that study, 11 samples showed an average PO_4 background concentration of 0.469 ± 0.051 mg PO_4 /g sediment, which was very close to the PO_4 analysis of a physically composited background sample. Phosphate was measured by a Hach 8178 method (Szecsody et al. 2007) and additionally by inductively coupled plasma (ICP) analysis of P. Citrate did not interfere with the PO_4 measurement. In this study, this background PO_4 value was used as a constant for all reported phosphate values, as measured by the Hach 8178 method. It should be noted that although the variability of this background value was small (i.e., 11% of the average), there is a small correlation between phosphate with grain-size distribution. In this study, because there were sediment zones containing predominantly silt and clay, additional phosphate background samples were evaluated for different sediment grain-size distributions (Figure 3.2). These data showed that with finer grained sediments that have higher surface area, somewhat greater phosphate is extracted. For an endpoint (the 300 Area less than 53 micron sieved fraction, Figure 3.2), the extracted phosphate was 1.5 mg/g. None of the 100-N Area sediments with high phosphate were this fine a grain size (most were fine sand with silt/clay). The reported phosphate values that ranged up to 10 mg PO_4 /g

could, therefore, only be partially attributed to somewhat higher background phosphate (only up to 1.0 mg/g, as shown in the 100-N Area sieved sediment fractions, Figure 3.2). Therefore, the reported phosphate values in this report for fine-grained sediment do represent real values.

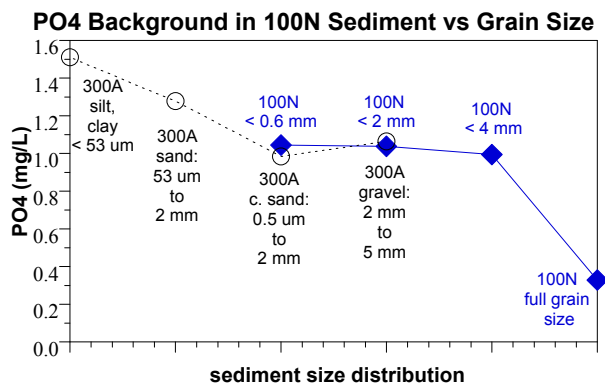


Figure 3.2. Phosphate Extraction from Sediment by Acid Dissolution for Different Grain-Size Distributions

Chemical extractions were also conducted to measure the ion exchangeable Sr-90 (0.5M Mg(NO₃)₂ extraction for 1 hour) and an acid extraction to dissolve the apatite to measure the Sr-90 incorporated into the apatite structure 0.5M HNO₃ for 15 minutes. Ion exchangeable and acid extraction of Sr-90 from subsurface sediments prior to any Ca-citrate-PO₄ injections show that approximately 90% of the Sr-90 is held on sediments by ion exchange, and is easily removed with the high ionic strength solution even after decades of contact time. The remaining 10% of the Sr-90 is hypothesized to be incorporated into carbonates (Heslop et al. 2005; Lazic and Vukovic 1991; Serne and LeGore 1996).

Sediment samples were also analyzed for ion exchangeable Ca²⁺ and Sr²⁺. These data are used to determine the amount of depletion of the divalent cations in the treatment zone relative to natural (pre-treatment) conditions, as characterized elsewhere (McKinley et al. 2007; Steefel 2004) with an average cation exchange capacity of 2.0 meq/100 g and 100-N Area sediments exchange sites 77.2% saturated in Ca²⁺, 16.8% Mg²⁺, 4.2% in K⁺, 2.7% in Na⁺, and 2.4% in Sr²⁺ (Szecsody et al. 2007). Depletion of both cations is indicative of the injection of the high ionic strength Ca-citrate-PO₄ water (high in Na) and ion exchange. Greater depletion of strontium relative to calcium is indicative of incorporation into apatite (Raicevic et al. 1996).

Ten sediment samples taken from the fish-bone apatite jet-injection area were analyzed for TOC to characterize how much organic matter was injected with the apatite. This analysis consists of a total carbon pyrolysis of the sediment at 900°C (both organic and inorganic carbon) and an inorganic carbon digestion by phosphoric acid at 200°C in a Shimadzu TOC-5000A carbon analyzer with solid sample module. Organic carbon content is the total carbon minus inorganic carbon content. The detection limit was 0.002% carbon, and analytical precision was 0.005%. Experiments were also conducted with the fish-bone apatite laden sediment to determine if the organic matter held more Sr-90 (Bellin and Rao 1993), then when the biomass died, the Sr-90 was released. These experiments consisted of parallel vials of sediment in clear glass vials in which some were kept in the dark (maintain subsurface conditions) and other vials were subjected to high intensity ultraviolet light for 240 hours (to kill most of the biomass). The total Sr-90, ion exchangeable Sr-90, and phosphate content was measured in the samples.

Scanning electron microscope (SEM) pictures with an energy dispersive x-ray spectroscopy (EDS) detector were used to identify apatite in a sediment sample from the Ca-citrate-PO₄ injection area sediment. Approximately 36 EDS spectra were obtained from different locations in the sediment. The identification of the mineral phase involves focusing the electron beam on the potential mineral (a few microns across) at high magnification (Figure 3.3a, b). This electron backscatter image shows that this crystal is likely precipitated apatite, as sediment grains are generally far larger and this small crystal is

located on the surface of a mineral grain (Moore et al. 2007). An EDS detector scan of this grain (Figure 3.3c) with peaks clearly shows the crystal structure is apatite.

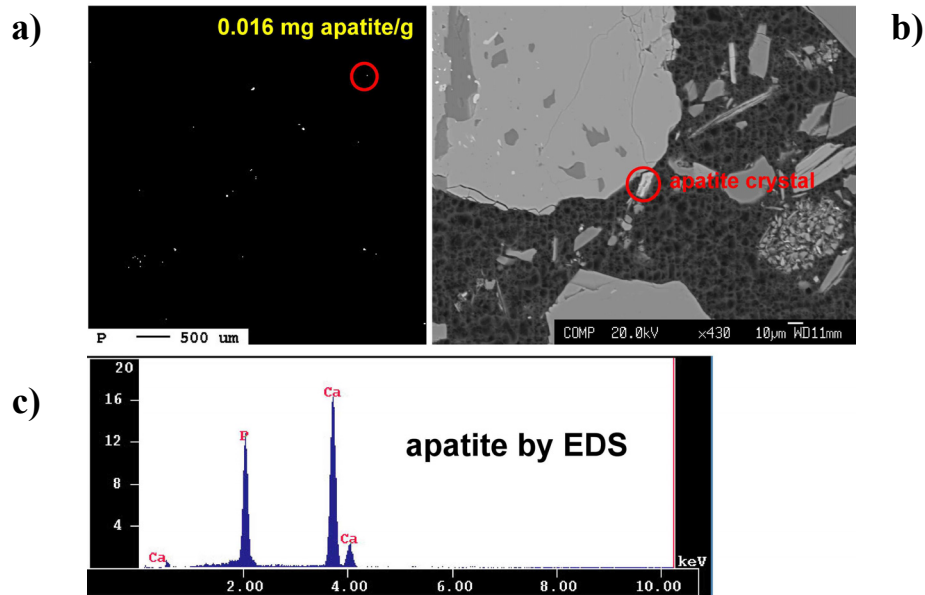


Figure 3.3. a) Mineral Phase Identification of a Location with High Phosphorous Concentration; b) Electron Backscatter of the Location is Indicative of a Surface Precipitate, with c) Identification of this Mineral as Apatite by Comparison to an Apatite Standard

3.2 Physical Analysis of Cores: Grain-Size Distribution, K_{sat}

Dry sieve analysis of sediment cores was conducted to determine the grain-size distribution. Sediment in the entire 6-inch core was first dried (45°C), then subjected to sieve analysis (12 sieves, 50 mm to 0.053 mm). The 20 grain-size distributions on the four boreholes are in the appendix. Three methods were used to calculate the saturated hydraulic conductivity from the grain-size distribution, although the K_{sat} value considered the most accurate (and used on graphs) is the modified Masch and Denny (1966) method. The simplest empirical relation is Hazen’s formula:

$$K_{sat} \text{ (cm/s)} = 1.0 (d_{10})^2 \quad (3.1)$$

where the 10% passing grain size (d_{10}) is in millimeters. This formula was originally determined for uniformly graded sands in the late 1800s. A “modified Hazen’s formula” was empirically derived from the relationship between grain-size distributions and measured saturated hydraulic conductivity measurements for various Hanford sediments

$$K_{sat} \text{ (cm/s)} = 0.0961 (d_{25})^{1.6624} \quad (3.2)$$

where the 25% passing grain size (d_{25}) reflects some of the grain-size mixture in Hanford sediments (as opposed to uniform porous media of the Hazen formula). The third empirical formula uses additional

points of the grain-size distribution, so more accurately reflects the influence of a range of grain sizes on flow. The modified Masch and Denny (1966) formula used in this study is

$$K_{\text{sat}} \text{ (cm/s)} = 0.0177 (d_{50}/\text{std dev})^{1.4319}; \text{ std dev} = [d_{16} - d_{84}]/4 + [d_5 - d_{95}]/6.6 \quad (3.3)$$

where the grain sizes are on a phi (ϕ) scale (Folk 1974)

$$\phi = -\log(\text{mm})/\log(2) \quad (3.4)$$

A continuous function was used to fit the log grain-size distribution in order to accurately calculate the grain-size percentages needed to estimate hydraulic conductivities from these empirical formulas. Grain-size distributions that exhibited multi-modal character (about half of the core samples) were fit with a more complex two-piece function.

4.0 Results for Groundwater Injection Area

4.1 Phosphate Mass in Cores

The target apatite concentration (1.7 mg apatite/g of sediment) corresponds to a pore volume amendment of 90 mM of phosphate precipitated in sediment with no retardation, or 45 mM phosphate precipitated with a retardation of 2.0. Laboratory and field Ca-citrate- PO_4 injections have demonstrated that phosphate retardation is in the range of 1.6 to 2.4, and dependent on the injection rate (i.e., due to slow PO_4 removal from solution by adsorption and precipitation).

Given the 10 mM PO_4 and 40 mM PO_4 injections in 100-N Area wells, an average apatite loading of 1.9 mg apatite/g of sediment (0.608 mg PO_4 /g) is expected. There may be higher concentrations near the injection wells and lower concentrations at greater distance from the injection wells.

Phosphate was analyzed in 45 samples at different depth (15 in each of 3 boreholes, Figures 4.1 through 4.3) using the less than 4 mm grain-size fraction, and in 18 samples at different depth (6 in each borehole) using the full grain-size fraction. The phosphate was extracted from the sediment with a weak acid (0.5M HNO_3 for 15 minutes), as established in previous studies (Szecsody et al. 2007, 2008), where the natural phosphate extracted from minerals in the untreated sediment (i.e., baseline phosphate) is accounted for.

Average phosphate for three boreholes (both Hanford formation and Ringold Formation) was 0.415 ± 0.232 mg PO_4 /g of sediment, or 68% of the target of 0.608 mg PO_4 /g of sediment (equivalent to 1.9 mg apatite/g). The Hanford formation received an average of 0.559 ± 0.253 mg PO_4 /g (92% of target) and the Ringold Formation received an average of 0.268 ± 0.113 mg PO_4 /g (44% of target).. These reported values are based on extraction from the whole grain-size

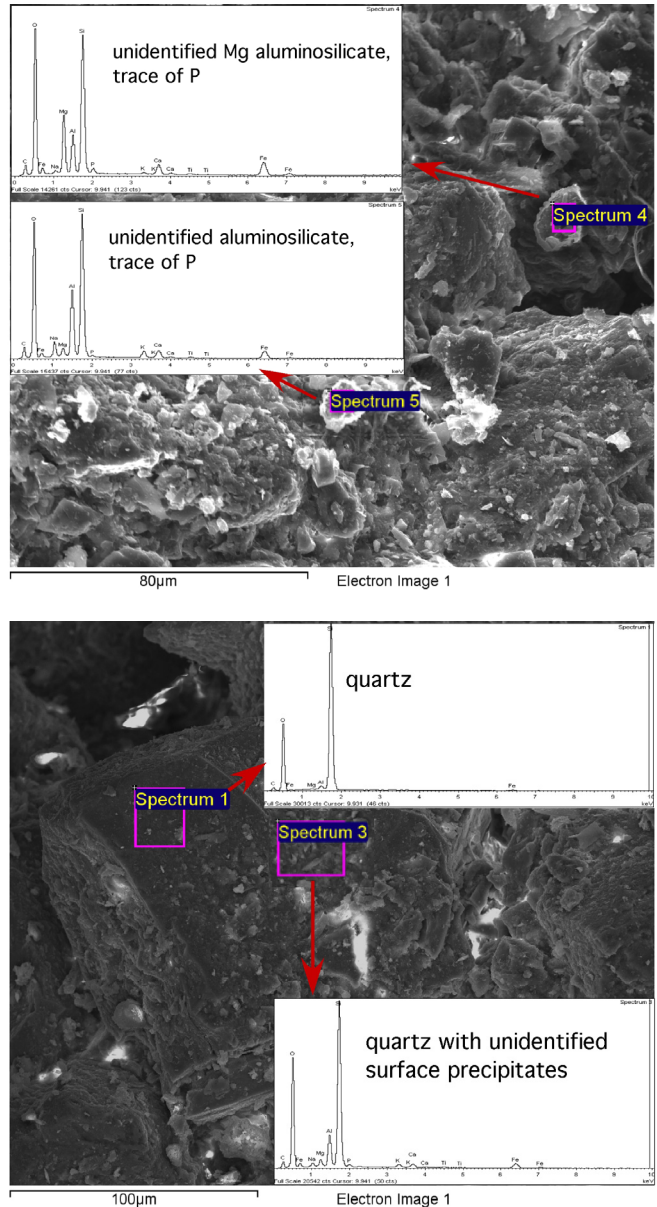


Figure 4.1. Scanning Electron Microscope Pictures of Sediment with Identification of Minerals by EDS Detector

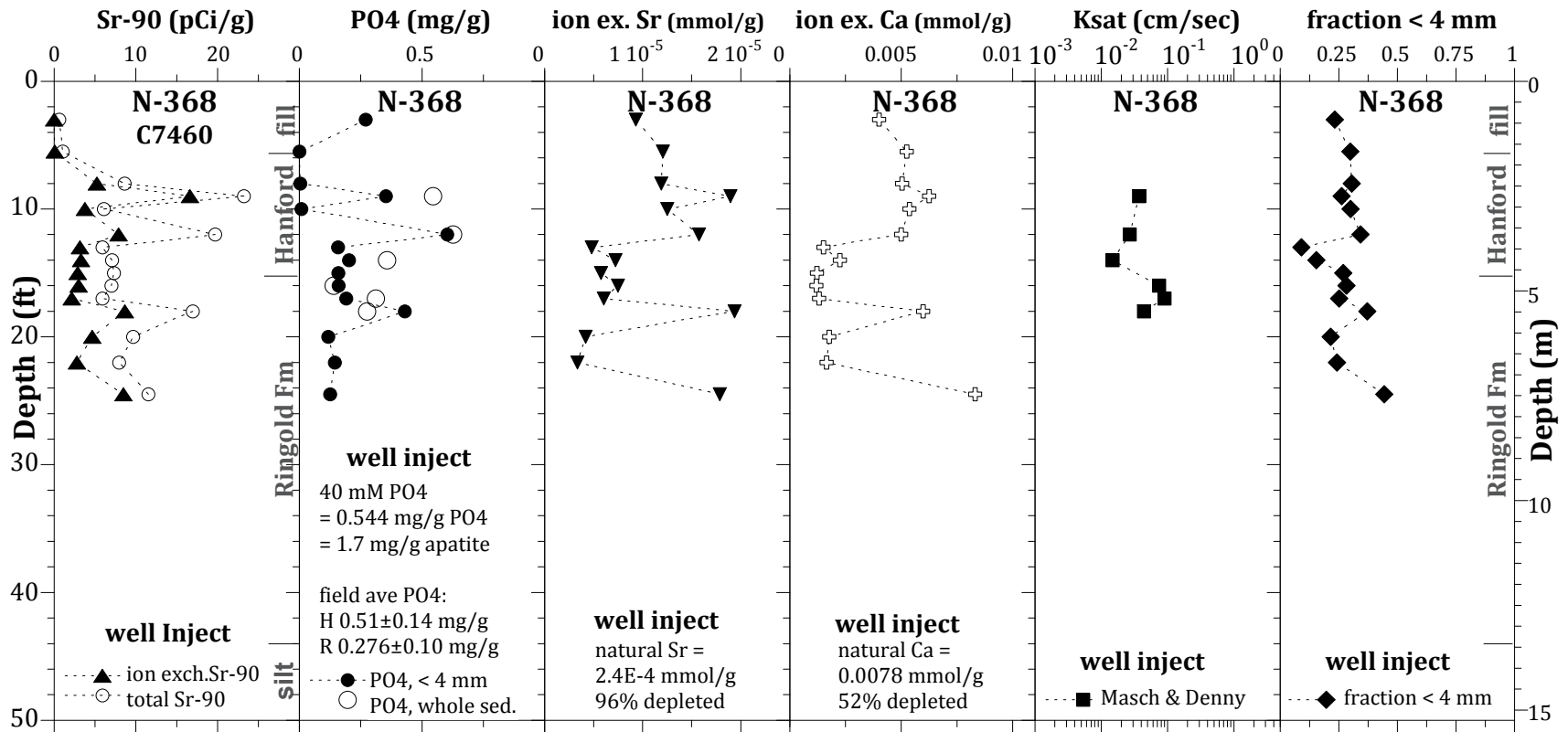


Figure 4.2. N-368 Vertical Profiles of a) Sr-90, b) PO₄, c) Ion Exchangeable Strontium, d) Ion Exchangeable Calcium, e) Calculated Saturated Hydraulic Conductivity (from grain-size distributions), and f) Fraction Grain Size less than 4 mm

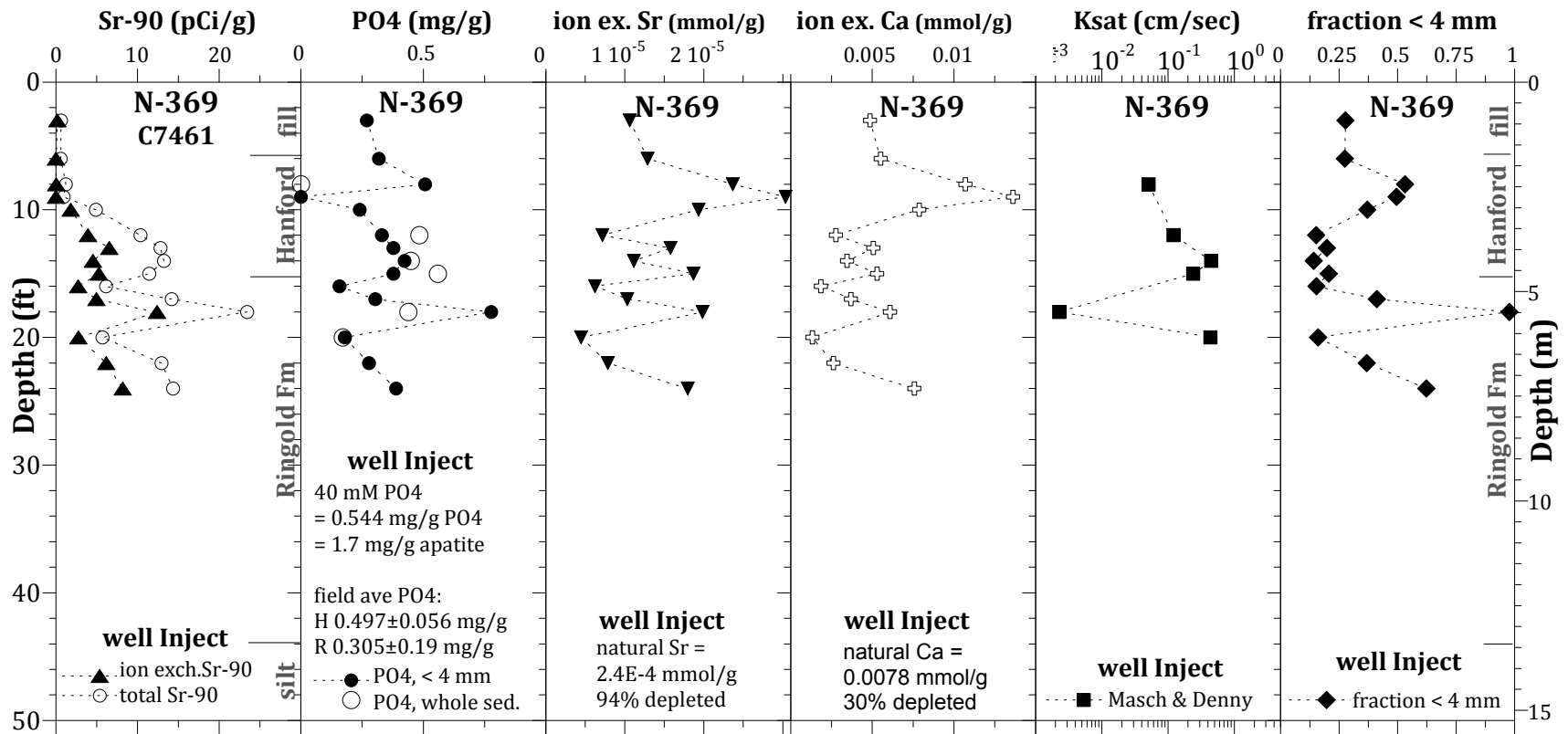


Figure 4.3. N-369 Vertical Profiles of a) Sr-90, b) PO₄, c) Ion Exchangeable Strontium, d) Ion Exchangeable Calcium, e) Calculated Saturated Hydraulic Conductivity (from grain-size distributions), and f) Fraction Grain Size less than 4 mm

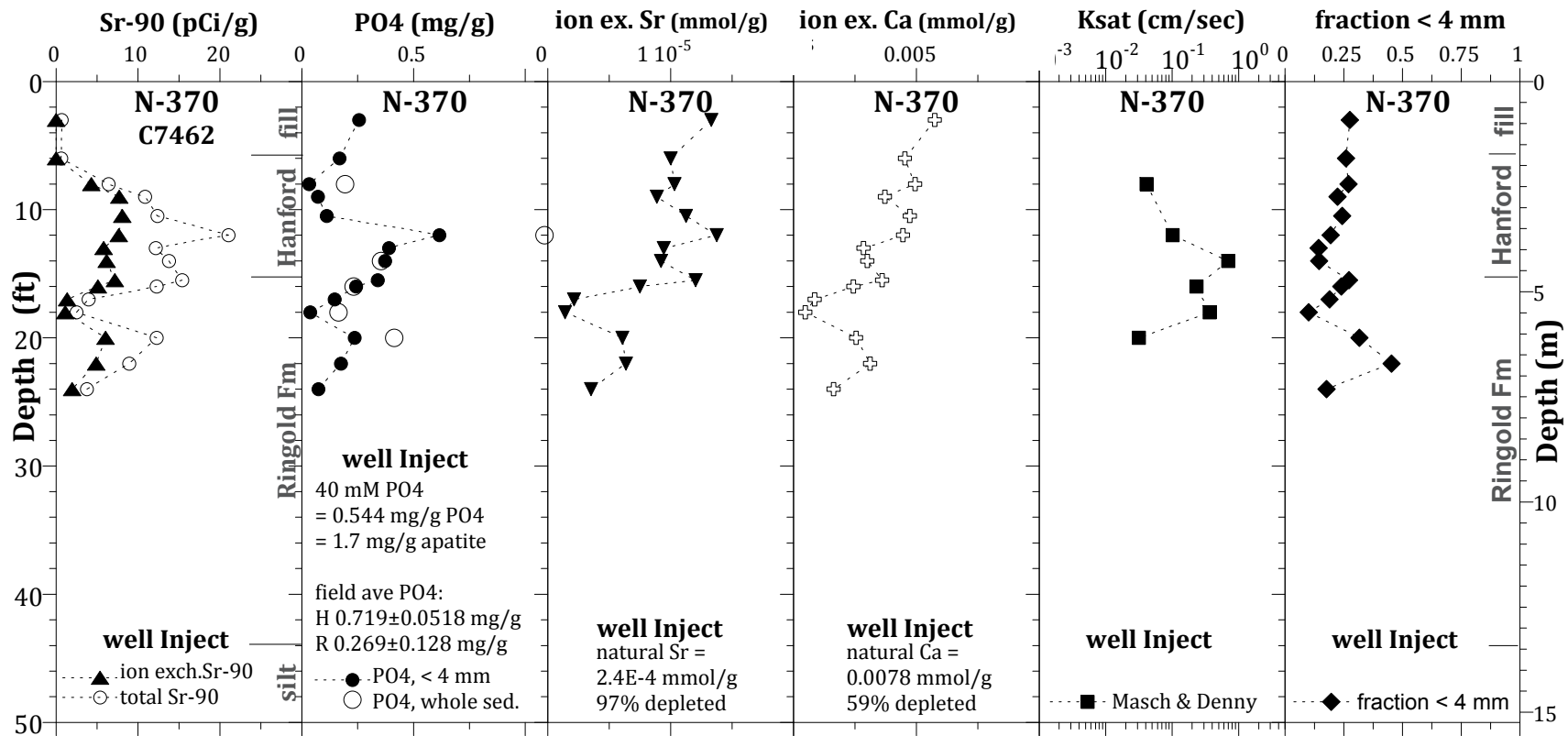


Figure 4.4. N-370 Vertical Profiles of a) Sr-90, b) PO₄, c) Ion Exchangeable Strontium, d) Ion Exchangeable Calcium, e) Calculated Saturated Hydraulic Conductivity (from grain-size distributions), and f) Fraction Grain Size less than 4 mm

distribution (1.0 to 2.0 kg per sample). Phosphate extractions on the less than 4 mm grain size averaged 17% lower (normalized to the PO₄ in the whole grain-size distribution).

Although these boreholes were located at different distances from injection well N-137 (i.e., 6.5 ft for N-368, 10.0 ft for N-369, and 15.7 ft for N-370), the average phosphate concentration was relatively constant (Table 4.1) at 0.376 mg/g (N-368), 0.420 mg/g (N-369), and 0.406 mg/g (N-370). This is not surprising, as the solution takes 50 to 200 hours (half-life) for citrate biodegradation, then Ca-PO₄ precipitation occurs.

Table 4.1. Average Phosphate Concentration in Groundwater Injected Boreholes

borehole	injection	average PO ₄ * (mg/g)	fill PO ₄ * (mg/g)	Hanford Fm PO ₄ * (mg/g)	Ringold Fm PO ₄ * (mg/g)	distance to PO ₄ injection (ft)	distance to additional PO ₄ injection wells (ft)
groundwater injection of Ca-citrate-PO₄							
N-368	Ca-citrate-PO ₄	0.376 ± 0.180	0.092±0.155	0.510±0.138	0.276±0.099	6.5	23.0
N-369	Ca-citrate-PO ₄	0.420 ± 0.147	0.365±0.126	0.497±0.056	0.305±0.189	10.0	17.0
N-370	Ca-citrate-PO ₄	0.406 ± 0.346	0.193±0.085	0.719±0.518	0.269±0.128	15.7	9.5

* using average background PO₄ = 0.46 mg/g

Within both the Hanford formation and the Ringold Formation, there is spatial variability of the measured PO₄ concentration (Figures 4.2b through 4.4b). In most cases, high phosphate at that depth corresponds to high total Sr-90 values (Figures 4.2a through 4.4a). In addition, low phosphate at a specific depth also generally corresponds to low total Sr-90. It is hypothesized that this correlation between PO₄ and Sr-90 concentration is related to lower hydraulic conductivity zones (with higher strontium adsorption and higher surface area) in the formation. Another hypothesis is that higher background phosphate in the finer-grained sediments leads to higher sorption and precipitation of Sr-90 (described in Section 3.1). Because Sr-90 disposal was inland, migration to this near-river location occurred by both vertical and horizontal migration, generally during high water flux from the disposal trenches. Therefore, moderate to high-K flow channels received the greatest mass flux of Sr-90. During Ca-citrate-PO₄ injections in fully screened wells, more PO₄ is also injected into the moderate- to high-K zones. Although low-K zones likely have higher sorption of Sr-90 and PO₄, there may be insufficient flow into these zones for the Sr-90 (during the less than 20 years of transport time) and PO₄ (injection time of days) to accumulate in them.

A sediment sample from borehole N-368, 12-ft depth, was analyzed using an EDS detector on a SEM to identify surface phosphate precipitate crystal structure. Previous studies using an electron microprobe and elemental detectors were able to positively identify that Ca-citrate-PO₄ solution precipitate in the Hanford Site 100-N Area sediment did produce apatite (as shown in Figure 3.3). Phosphate precipitates occur in small less than 50 micron conglomerates of finer grained precipitate at a low concentration (less than 0.5 mg/g of sediment). Of a total of 36 EDS spectra, 17 showed trace phosphorous on the sediment surface (Figure 4.1), but apatite crystal structure was not positively identified, as in an earlier study (shown in Figure 3.3c).

4.2 Sr-90 Distribution in Cores

Sr-90 (and strontium) behaves nearly the same as calcium in the Hanford Site 100-N Area subsurface, so it is primarily adsorbed by ion exchange to sediments. The retardation factor for strontium (and Sr-90) under natural groundwater conditions is approximately 125, meaning 125 times more strontium mass is held on the surface than is in groundwater. Even after decades of Sr-90 contact with the sediment, approximately 90% is easily desorbed using a high ionic strength (ion exchange) solution. A similar conclusion was reached in a previous study (Serne and LeGore 1996). Therefore, sorbed Sr-90 has a high potential for mobilization. The ion exchangeable strontium is easily desorbed by the injection of a solution of higher ionic strength water (such as spills and the Ca-citrate-PO₄ injection solution).

The total Sr-90 in the sediment (open circles, Figures 4.2a, 4.3a, and 4.4a) vary with depth. The ion exchangeable Sr-90 (triangles, Figures 4.2a, 4.3a, and 4.4a) are approximately half of the total Sr-90 in zones of PO₄ treatment. More specifically, the fraction of ion exchangeable to total Sr-90 in the Hanford formation averages 50.9%, the Ringold Formation averages 50.3%, and the fill (0- to 8-ft depth) averages 77%. Therefore, the Hanford and Ringold Formations average 39.4% Sr-90 incorporation into apatite by 1 year (given that untreated sediment has 90% ion exchangeable Sr-90 minus the 50% ion exchangeable for treated sediment). It is expected that additional Sr-90 will be incorporated into apatite in the subsequent years, because Sr-apatite is thermodynamically more stable than Ca-apatite. Although, on average 50.6% of Sr-90 is still adsorbed by ion exchange on sediment and apatite, the retardation of Sr-90 has changed. Sr-90 adsorption to apatite ($K_d = 1375$ mL/g, $R_f = 6800$) is 55 times stronger than to sediment ($K_d = 25$ mL/g, $R_f = 125$).

For the first process (ion exchange), the system is temporarily not at equilibrium (i.e., the injection zone has excess Na⁺ and is deficient in the divalent cations (including Sr²⁺ and Ca²⁺). Over time (a few years), upgradient cations invade the zone and equilibrium is slowly approached. Therefore, for several years, a temporary strontium/calcium deficient zone is created. To date, Sr-90 (aqueous) measured in groundwater is significantly lower than pre-injection conditions (Vermeul et al. 2010). To determine the fraction that was caused by the ion exchange versus sorption to apatite versus incorporation in apatite, several different analyses were conducted.

The more stable or permanent sequestration that occurs with the addition of apatite is the incorporation of Sr-90 into the apatite structure. This process occurs slowly over time. Assuming equilibrium cation exchange to both the sediment and apatite (Gaines-Thomas activity convention) with a single site on each surface, the fraction of Sr-90 was calculated on sediment and on apatite with different apatite loadings (Table 4.2). This calculation assumes no incorporation of Sr-90 into apatite. With no apatite (case #1, Table 4.2), 99% of the Sr-90 is sorbed to sediment and 0.79% is aqueous (and total $R_f = 125$). With an apatite loading of 1.7 mg apatite/g of sediment (case #3, Table 4.2), 8.3% of the Sr-90 is sorbed to apatite, and 91% to sediment (and total R_f increased slightly to 136.5). The distribution of Sr-90 mass at 1 year is 39.4% incorporated into apatite, 45.6% adsorbed to sediment 5% adsorbed to apatite, and less than 0.7% aqueous. Therefore, there is only a minor decrease in aqueous Sr-90 adsorption due to the presence of apatite; the slow incorporation of Sr-90 into the apatite structure is the major process causing sequestration of Sr-90. Due to the high concentration injections of Ca-citrate-PO₄, the sediment system is far from equilibrium conditions, in terms of major divalent cations (Ca, Mg, Sr), as described in a following section. This has some short-term influence on the observed aqueous Sr-90 concentrations.

Table 4.2. Calculated Sr-90 Adsorption to Sediment in Apatite in Mixed Systems

#	Kd, apa. (cm ³ /g)	Kd, sed. (cm ³ /g)	apatite mass (g)	sediment mass (g)	volume (mL)	ion exchange equilibrium				total Kd (mL/g)	total Rf
						fraction aqueous	frac. sorbed on apatite	frac. sorbed on sediment	frac. sorbed total		
field sediment/water ratio: 20% porosity											
1	1350	25	0	1.0	0.2	0.0079	0.0000	0.9921	0.9921	25.0	125.0
2	1350	25	0.00038	1.0	0.2	0.0078	0.0200	0.9723	0.9922	25.5	127.6
3	1350	25	0.0017	1.0	0.2	0.0073	0.0835	0.9093	0.9927	27.3	136.5
4	1350	25	0.0038	1.0	0.2	0.0066	0.1691	0.8243	0.9934	30.1	150.6

4.3 Ion Exchangeable Calcium and Strontium

In addition to the accumulation of Sr-90 (and Sr) in apatite by adsorption/incorporation into the apatite structure, ion exchange during the initial Ca-citrate-PO₄ solution injection has also altered the cations on the sediment ion exchange sites from their natural condition. The natural sediment has 2.04 meq of ion exchange sites/100 g (Szecsody et al. 2007) that are occupied with Ca²⁺ (77.2%), Mg²⁺ (16.8%), K⁺ (4.2%), Na⁺ (2.7%), and Sr²⁺ (2.4%). The high concentration Ca-citrate-PO₄ solution cation composition of 3.6 mM Ca²⁺, 4.0 mM NH₄⁺, and 100.4 mM Na⁺. Although a monovalent ion (Na⁺) does not efficiently exchange off all of the divalent cations (i.e., Ca²⁺, Mg²⁺, Sr²⁺), some ions are exchanged off due to the high Na⁺ concentration. In addition, the Ca-citrate-PO₄ injection solution was deficient in Ca-citrate in order to utilize sediment ion exchangeable Ca²⁺ and Sr²⁺ for precipitation.

Analysis of the ion exchangeable Ca²⁺ and Sr²⁺ from the field cores (Figures 4.2c, d through 4.3c, d) clearly show significant depletion in both Sr²⁺ (average 95% lower concentration relative to natural sediment) and Ca²⁺ (average depletion 47%). Because Sr²⁺ and Ca²⁺ geochemical behavior is nearly the same, the amount of depletion caused by the high ionic strength flushing should be the same. The much greater depletion in Sr²⁺ compared to Ca²⁺ is likely due to incorporation into apatite. Therefore, this ion exchange analysis shows that Sr²⁺ adsorption on the sediment surface is approximately 5% of natural values, so it is expected that groundwater Sr²⁺ (and Sr-90 values) will reflect similar 95% depletion.

4.4 Grain-Size Distribution and Hydraulic Conductivity

The saturated hydraulic conductivity was calculated from grain-size distributions of 18 cores (grain-size distributions shown in the appendix), as shown in Figure 4.2e through 4.4e. In addition, the fraction grain size less than 4 mm (Figures 4.2f through 4.4f) also show locations of low K zones. Grain-size distributions for boreholes N-368 and N-370 show relatively even distributions with depth (Figure 4.5a), and N-369 shows a low-K zone at an 18-ft depth (Figure 4.6a).

The total Sr-90 and extracted PO₄ data (Figures 4.2 through 4.4) show good correlation, which suggests less permeable zones in which the Sr-90 advected into (and the Ca-citrate-PO₄ solution was injected into) that have greater Sr-90 adsorption are the cause of the correlation. Calculated hydraulic conductivity measurements on approximately half of a core (1 to 2 Kg of sediment) and subsequent calculated saturated hydraulic conductivity were not correlated with Sr-90 (Figure 4.5a), and PO₄ (Figure 4.5b). It is suspected that this lack of correlation with the laboratory K_{sat} values is caused by the measurement being made on too small of a sample. Field-scale electronic borehole flow meter tests to determine the relative hydraulic conductivity at a somewhat larger scale in the field may yield the presumed correlation with Sr-90 and phosphate. The fact that there is a fair correlation between the total

Sr-90 and the extractable phosphate in the sediment (Figure 4.6b, $R = 0.82$) appears to indicate an underlying mechanism and correlation with hydraulic conductivity. It should be noted that over time (decades) the apatite accumulates Sr-90 in its structure, so this correlation will become stronger as up gradient Sr-90 flows into the apatite-laden zone. At this time of 1 year after phosphate emplacement, little additional Sr-90 would have been advected into this zone.

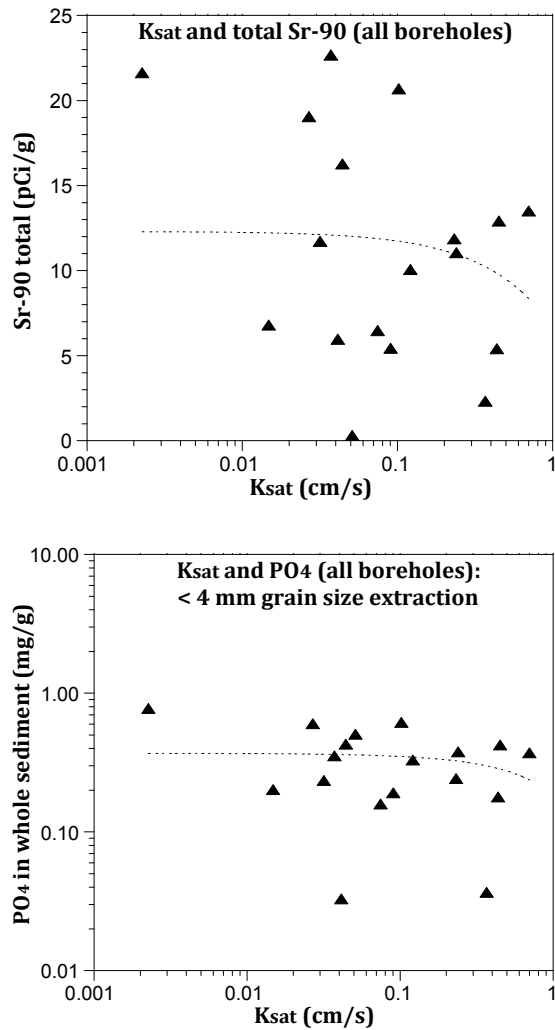


Figure 4.5. Correlation Between Saturated Hydraulic Conductivity and a) Total Sr-90 and b) PO_4 in Sediment

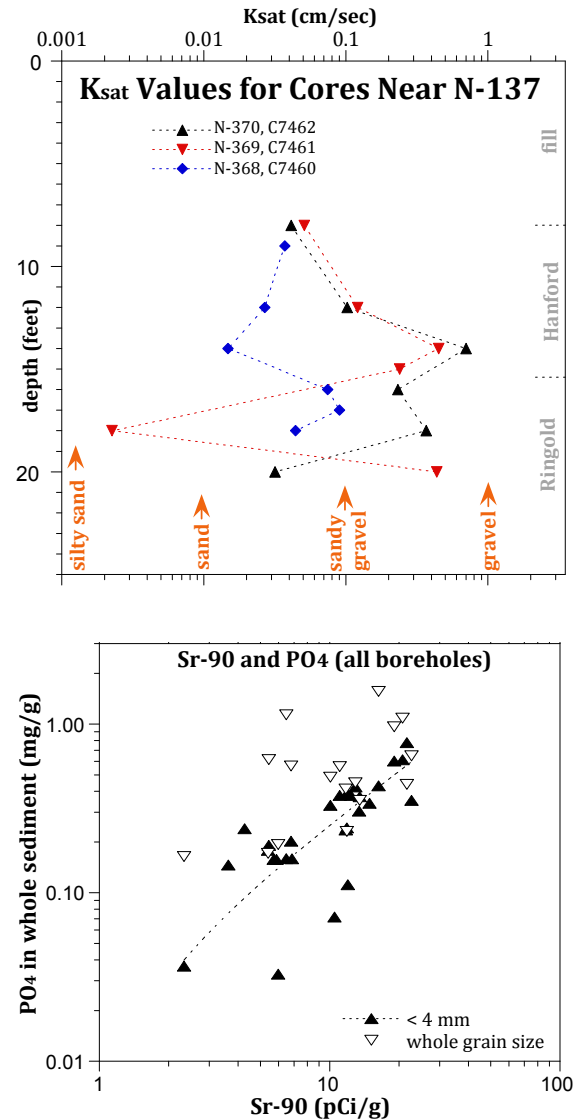


Figure 4.6. Correlation of Total Sr-90 and Phosphate in Sediment Cores

4.5 River Sediment Sample Analysis

Two river sediment samples were taken by Washington Closure Hanford, LLC that represent sediment in the 100-N Area (N outfall, Table 4.3) and a sediment sample near the high concentration Sr-90 plume (T100N3a; 200 ft NW of N-138). The total Sr-90 in the N Outfall sample was 1.8 pCi/g, which was similar to most depths from N-217, N-219, N-220, and N-222 with a mixture of fine and coarse materials. Finer grained depths from those boreholes were as high as 6 pCi/g total Sr-90 (acid extraction). There was a background amount of phosphate in the samples (less than 0.2 mg/g).

Table 4.3. River Sediment Analysis

sample	% water (g/g)	Sr-90 ion exch. (pCi/g)	Sr-90 total (pCi/g)	PO4* (mg/g)	size fraction < 4 mm
T100N3A	0.036	0.05	0.66	0.12	0.138
N Outfall	0.045	0.74	1.77	0.20	0.447

5.0 Results in Jet Core Injection Area

Geochemical and physical data from jet-injected cores are presented as depth profiles for each borehole (Figures 5.1 through 5.4) in order to illustrate correlations between grain size and Sr-90 and phosphate content.

5.1 Phosphate Mass in Cores

The phosphate content in sediment samples was measured in approximately 15 vertical locations for each borehole (Figures 5.1b to 5.4b), with averages for each borehole in Table 5.1. Borehole N-217 (Figure 5.4b), which was water jetted with sodium phosphate only, had an average of 1.2 mg PO₄/g of sediment, whereas N-222 (water jetted with fish bone only; Figure 5.1b) had an average of 1.63 mg PO₄/g. The two other boreholes (N-219 and N-220), which were water jetted with both sodium phosphate and fish-bone apatite, averaged 1.76 mg PO₄/g. Therefore, jetting in fish-bone apatite achieved somewhat greater phosphate mass than jetting in sodium phosphate. The target apatite content of 1.7 mg apatite/g of sediment corresponds to 0.54 mg PO₄/g of sediment, so three boreholes showed an average PO₄ that achieved the target and N-220 (fish bone + PO₄ injection) was low at 0.8 mg PO₄/g.

The vertical variability in phosphate content in the four boreholes was considerable, with a standard deviation equal to 81% the average value (Table 4.1). In contrast, cores (N-368, N-369, and N-370) taken near Ca-citrate-PO₄ injection into N-137 have a standard deviation was 43% of the average. This high phosphate variability for the jet-injected cores may be caused by formation properties (i.e., finer grained sediments may be looser and easier to jet into) or partially by jetting operations such as ponding phosphate near the surface. Borehole N-220 showed a more even vertical distribution of phosphate (i.e., PO₄ standard deviation is 60% of the mean), in spite of the grain-size fraction less than 4 mm (Figure 4.2f), Sr-90 profile (Figure 5.2a), and ion exchangeable strontium and calcium indicating finer sediment at the 4-ft depth. Therefore, jetting operations of phosphate and fishbone apatite at this location are thought to have achieved a relatively uniform vertical phosphate distribution.

In contrast to N-220, boreholes N-217 (Figure 5.4) and N-219 (Figure 5.3) both showed very high phosphate concentrations (to 10 mg/g) in shallow sediments (less than 10 ft), with less than 1 mg/g at depth. The shallow sediment in both wells show fine sediment in the 4- to 8-ft depth (size fraction data, Figures 5.3f and 5.4f). The Sr-90, ion exchangeable strontium, and ion exchangeable calcium data also indirectly indicate fine sediment, with elevated values in this depth interval. There were fewer points for the calculated hydraulic conductivity, but a low K_{sat} value is at a 10-ft depth in N-217. During jetting operations, shallow trenches were apparently dug to capture phosphate-laden water to allow for infiltration. This would lead to elevated phosphate values in shallow sediment (and account for the observed PO₄ vertical profile in N-219). However, the phosphate vertical profile in N-217 shows elevated values at 4 ft and also at 10 ft (with low phosphate in between), which is not consistent with infiltration of phosphate-laden water. This PO₄ profile, however, is consistent with the grain-size distribution, with finer zones at the 4-ft and 10-ft depth. It is hypothesized that these zones may be easier to jet inject into than coarser-grained sediments, so received a greater mass of phosphate.

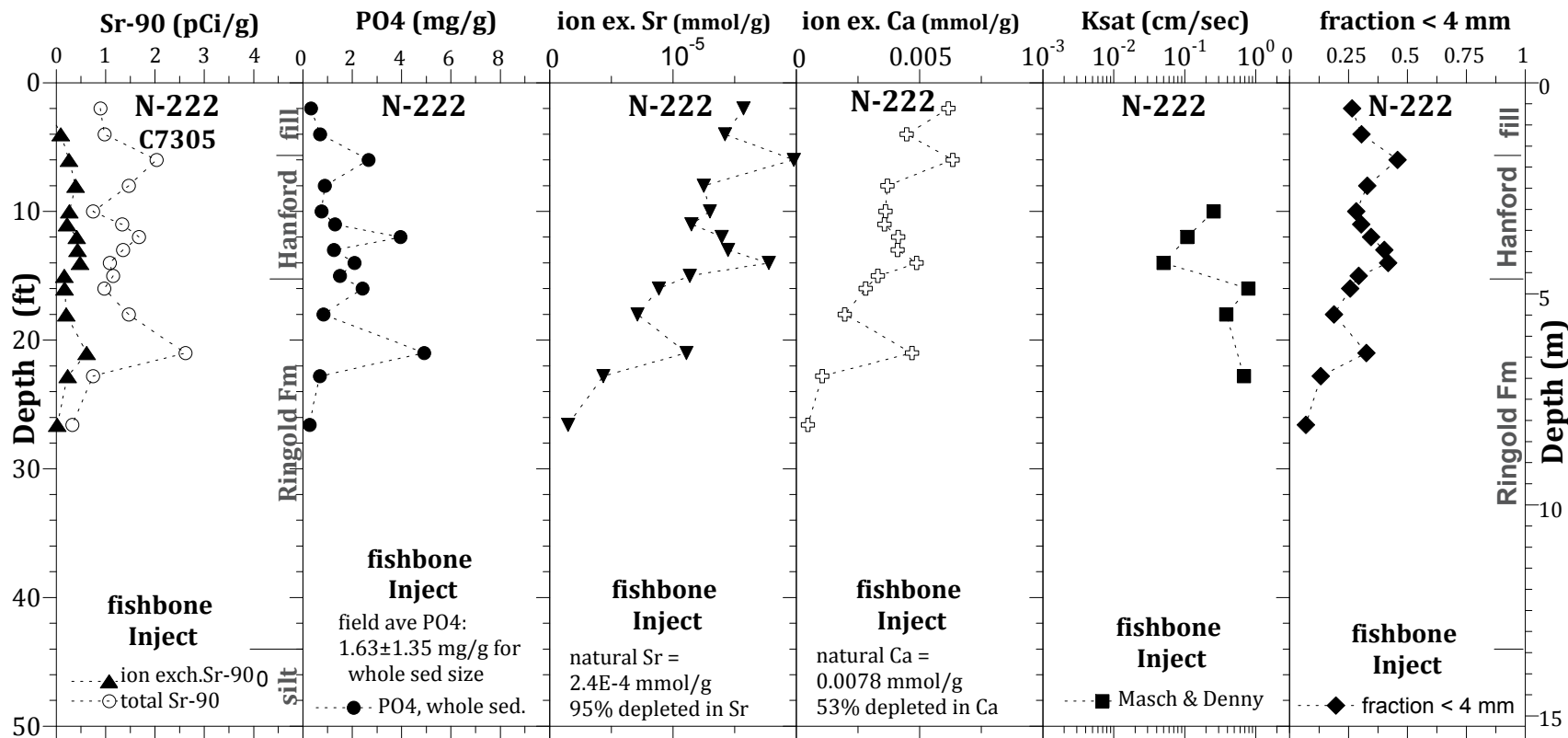


Figure 5.1. N-222 Vertical Profiles of a) Sr-90, b) PO₄, c) Ion Exchangeable Strontium, d) Ion Exchangeable Calcium, e) Calculated Saturated Hydraulic Conductivity (from grain-size distributions), and f) Fraction Grain Size less than 4 mm

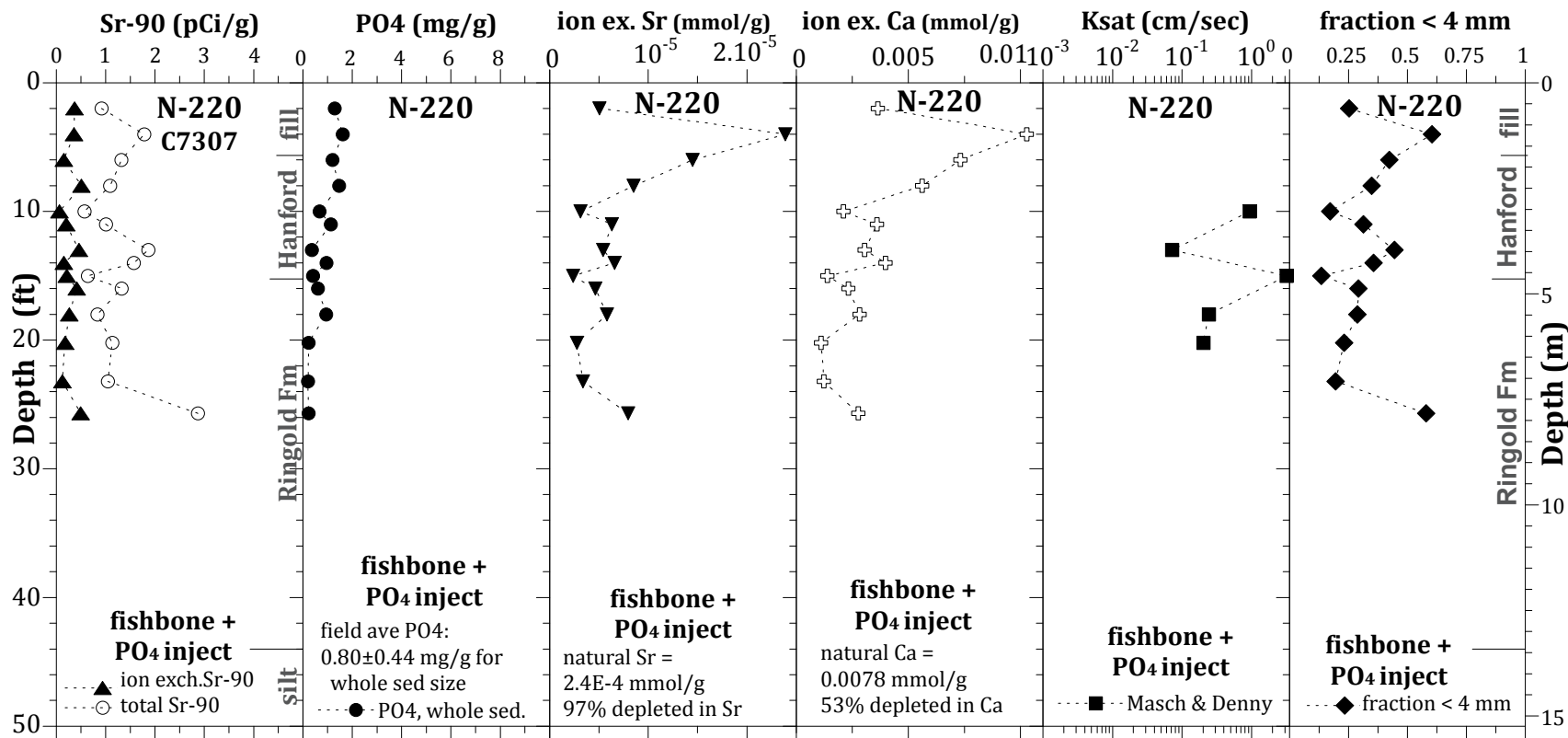


Figure 5.2. N-220 Vertical Profiles of a) Sr-90, b) PO₄, c) Ion Exchangeable Strontium, d) Ion Exchangeable Calcium, e) Calculated Saturated Hydraulic Conductivity (from grain-size distributions), and f) Fraction Grain Size less than 4 mm

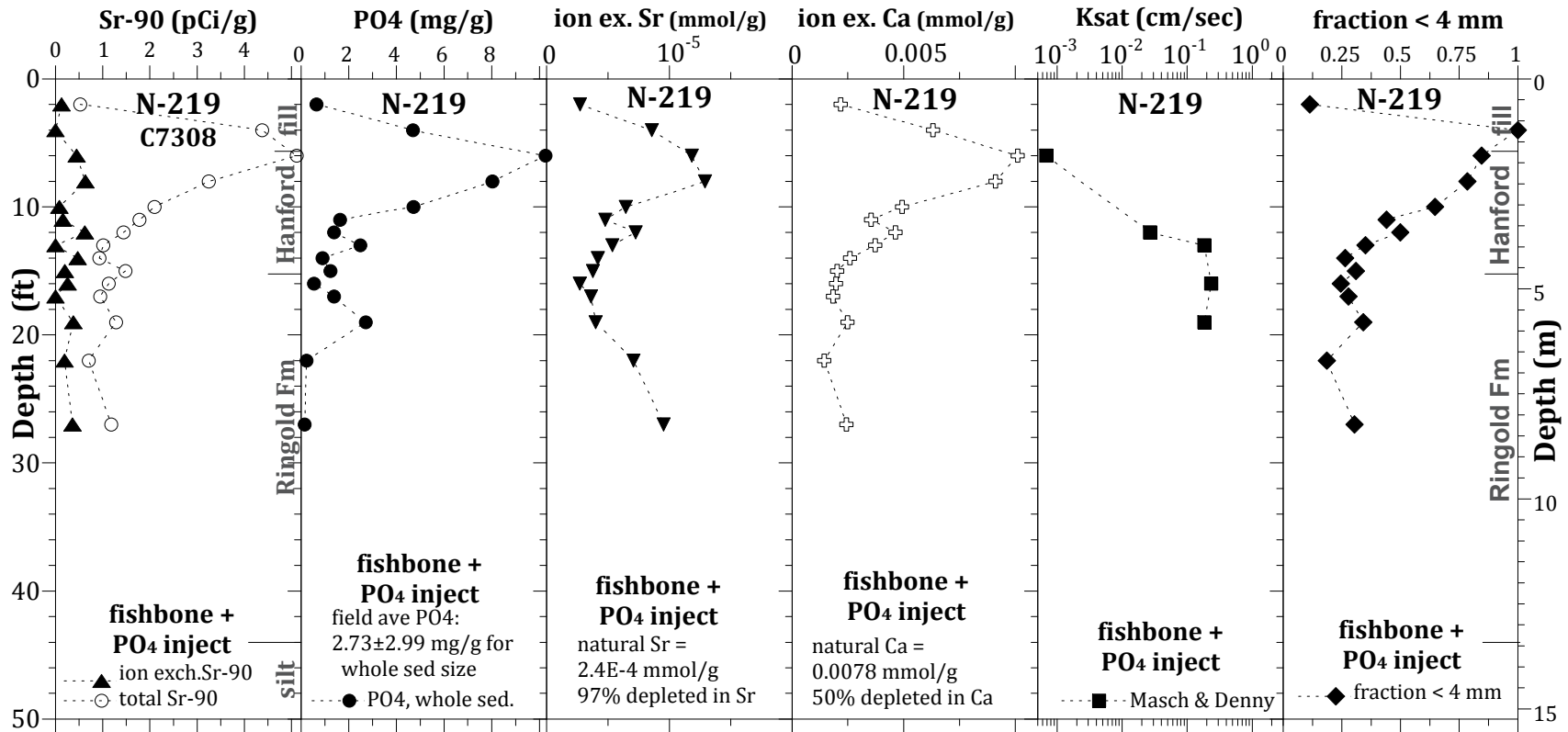


Figure 5.3. N-219 Vertical Profiles of a) Sr-90, b) PO₄, c) Ion Exchangeable Strontium, d) Ion Exchangeable Calcium, e) Calculated Saturated Hydraulic Conductivity (from grain-size distributions), and f) Fraction Grain Size less than 4 mm

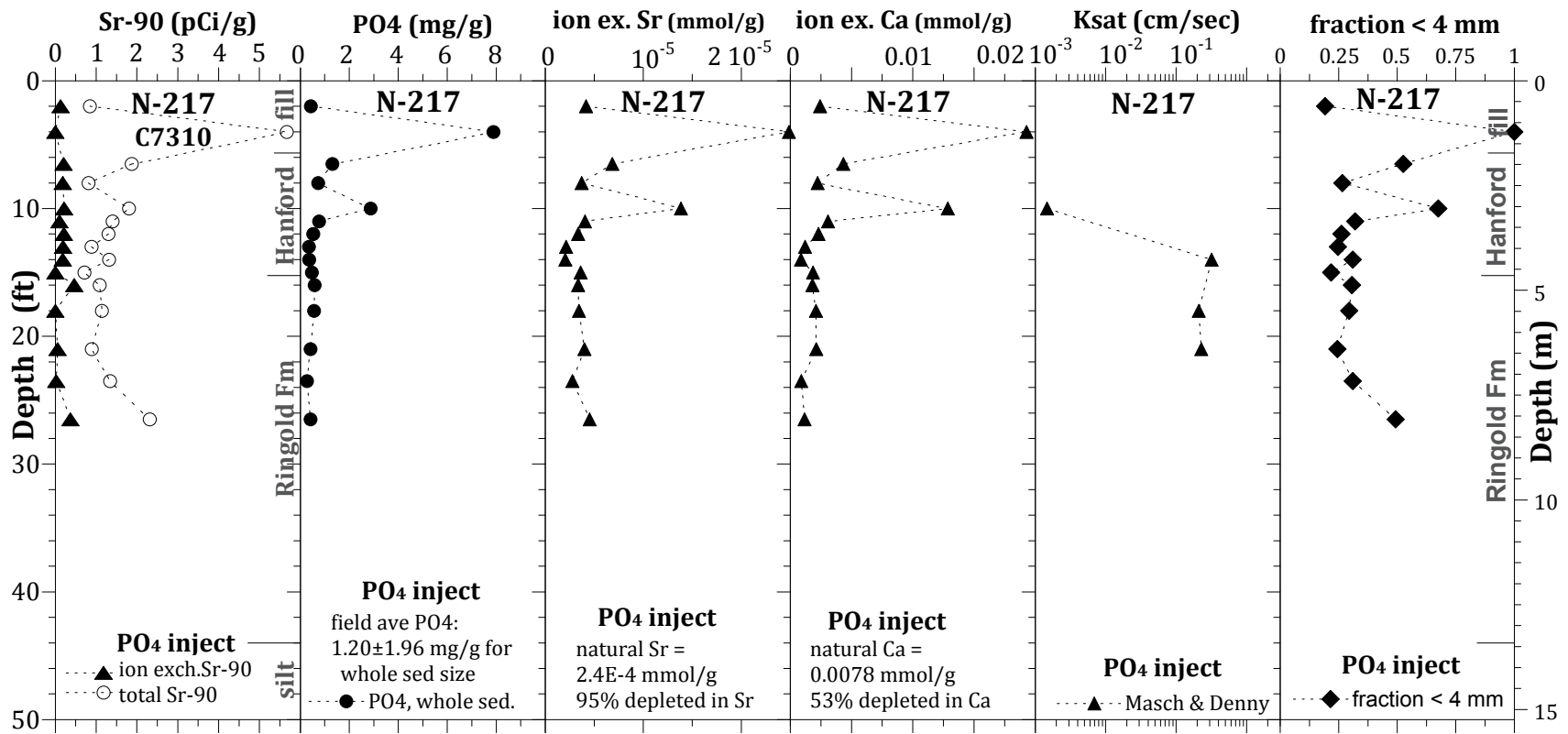


Figure 5.4. N-217 Vertical Profiles of a) Sr-90, b) PO₄, c) Ion Exchangeable Strontium, d) Ion Exchangeable Calcium, e) Calculated Saturated Hydraulic Conductivity (from grain-size distributions), and f) Fraction Grain Size less than 4 mm

Table 5.1. Phosphate Content in Water-Jet Injected Boreholes

borehole	injection	average PO ₄ * (mg/g)	fill PO ₄ * (mg/g)	Hanford Fm PO ₄ * (mg/g)	Ringold Fm PO ₄ * (mg/g)	distance to PO ₄ injection (ft)	distance to additional PO ₄ injection wells (ft)
jet injection of apatite and/or Na-PO₄							
N-222	apatite	1.63 ± 1.35	1.14 ± 1.04	1.81 ± 1.14	1.82 ± 1.91	0.99	5.1,5.3,5.8,6.0,8.4
N-220	PO ₄ , apatite	0.80 ± 0.48	1.39 ± 0.19	0.39 ± 0.30	0.40 ± 0.36	3.78	4.19, 7.57
N-219	PO ₄ , apatite	2.73 ± 2.99	5.90 ± 4.19	2.06 ± 1.41	1.00 ± 1.07	2.51	5.82, 7.44
N-217	PO ₄	1.20 ± 1.96	2.58 ± 3.55	0.89 ± 0.98	0.45 ± 0.13	1.06	3.7,5.2,6.4,9.1,11.4

* using average background PO₄ = 0.46 mg/g

Borehole N-222 showed three high zones of phosphate at the 6-ft, 11-ft, and 21-ft depth (Figure 5.1b). These depths do appear to correspond to finer grained sediment zones, as Sr-90, ion exchangeable calcium and strontium, and the fraction of sediment less than 4 mm were greater, as described earlier. Although there is a good correlation between elevated phosphate and mass fractions of finer grain sizes in all water-jet injected boreholes (Figure 5.5a), the high phosphate is mainly related to the water-jet injections, as the correlation does not exist for the groundwater-injected boreholes (Figure 5.5b, circles). Background phosphate is slightly elevated for silt/clay (0.69 mg PO₄/g above the background phosphate for sandy gravels), but this is too small to account for the high (up to 10 mg PO₄/g) phosphate values observed (described further in Section 3.1).

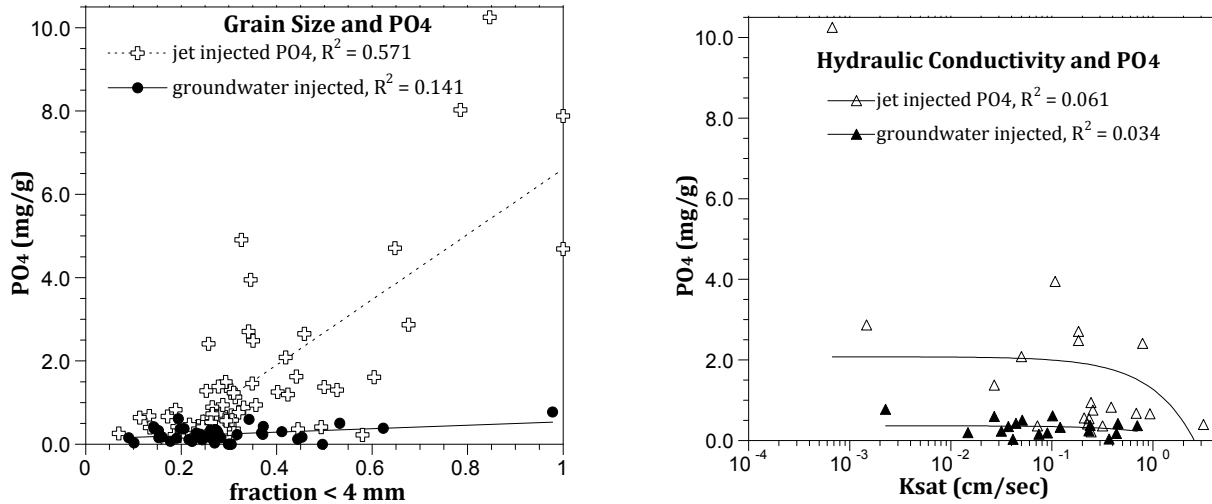


Figure 5.5. Correlation Between a) Grain Size and PO₄ and b) Saturated Hydraulic Conductivity and PO₄

5.2 Sr-90 Distribution in Cores

Sr-90 values in all four boreholes (Figures 5.1a through 5.4a) are all less than 5 pCi/g (total Sr-90), so considerably lower than the 90-pCi/g peak at a 15-ft depth in N-123, which is 230 ft to the northeast of N-222. All boreholes show that the ion exchangeable Sr-90 (black triangles) averages 18.1% (±14%) of the total Sr-90 (untreated sediment averages 90% ion exchangeable Sr-90), which appears to indicate

most of the Sr-90 is bound in apatite (by this indirect evidence). This hypothesis would have to be proven by electron microscope analysis to evaluate the Sr-90 content of apatite precipitates in the sediment.

Sorption and precipitation in sediments in which phosphate only (N-217) or phosphate and fish-bone apatite (N-219 and N-220) appeared to sequester more Sr-90 in apatite appeared to be largely controlled by the low-K zones with very high phosphate content. Injection of phosphate alone (to form apatite in situ) should lead to more rapid Sr-90 incorporation into apatite (compared with injection of fish-bone apatite, which has to slowly exchange calcium for strontium in the solid apatite). These borehole data are consistent with that hypothesis, as the average ion exchangeable Sr-90 fraction for N-217 (phosphate injection) was 0.12 ± 0.11 , with N-222 (fish-bone injection) at 0.20 ± 0.12 , and N-219 and N-220 (fish-bone and apatite injection) at 0.19 ± 0.16 and 0.23 ± 0.12 , respectively. Untreated sediment had a fraction ion exchangeable Sr-90 of 0.90.

5.3 Ion Exchangeable Calcium and Strontium

Ion exchangeable calcium and strontium were measured in sediment cores by a 1-M Mg-nitrate extraction (i.e., ion exchange solution) for 1 hour. The ion exchangeable calcium and strontium (Figures 5.1c, d through 5.4c, d) show similar vertical profiles as the Sr-90 data, because strontium (and Sr-90) geochemically behave nearly the same as calcium. Zones of a higher fraction of finer grained material (with higher surface area) had higher ion exchangeable calcium and strontium.

5.4 Grain-Size Distribution and Hydraulic Conductivity

Twenty cores were sieved (4 to 6 in each borehole) to obtain an approximate distribution of the change in hydraulic conductivity with depth. An indication of the grain size is shown in the less than 4-mm size fraction (Figures 5.1f through 5.4f). From the grain-size distributions (data and graphs in the appendix), the saturated hydraulic conductivity was calculated using the Masch and Denny (1966) method described earlier. Hydraulic conductivity values averaged 0.416 ± 0.695 cm/sec (average of log values, arithmetic average = 0.429 ± 0.441 cm/sec). Most values ranged between 0.02 to 0.5 cm/sec (average for a sandy gravel), with a few silt/clay zones ($K_{\text{sat}} = 7 \times 10^{-4}$ cm/sec), and a few clean gravel zones (K_{sat} up to 3.2 cm/sec), as shown in Figure 5.6. As shown earlier for each borehole, there were shallow fine-grained sediment zones. For these data shown, the Hanford formation had a slightly lower average hydraulic conductivity compared with the underlying Ringold Formation. In general, injections in the 100-N Area show approximately three times greater flow in the Hanford formation, so this may be an artifact of too few samples, or this specific area has somewhat different properties, or water-jet injections altered the hydraulic conductivity. Finer grained sediments (with higher surface area) showed elevated ion exchangeable strontium and calcium (Figures 5.1c, d to Figures 5.4c, d). Phosphate was also correlated with finer grained sediments, which appears to be an artifact of the water-jet injections and was not observed with Ca-citrate- PO_4 injections, as shown in Figure 4.5a.

5.5 Fish-Bone Organic Matter and Influence on Sr-90 Mobility

The influence of the organic matter associated with the fish-bone apatite is not well understood. Because biomass will grow on this organic matter (and the supplied phosphate source), there will be some utilization of calcium and strontium (and Sr-90). Once the organic matter is depleted, the biomass will

decrease, which could release Sr-90. What needs to be measured is how much Sr-90 is released upon biomass death in order to assess the significance of this process. Thirteen sediment samples were submitted for TOC analysis, and were not completed at the time of writing of this report. In order to assess how much Sr-90 is released upon biomass death, sediment experiments need to be conducted in which the biomass is killed without adding a chemical to the system. Addition of a bactericide (such as antibiotics or mercuric chloride) will lead to some ion exchange. Radiation or ultraviolet light can be used to kill microbes in the system without chemical addition. In one laboratory study in which microbial isolates were added to sediment (Bellin and Rao 1993), although sorption of two organic compounds increased, ion exchange of calcium did not change. The total biomass added was minimal (10^6 CFU/g), so there was little uptake of cations by microbes.

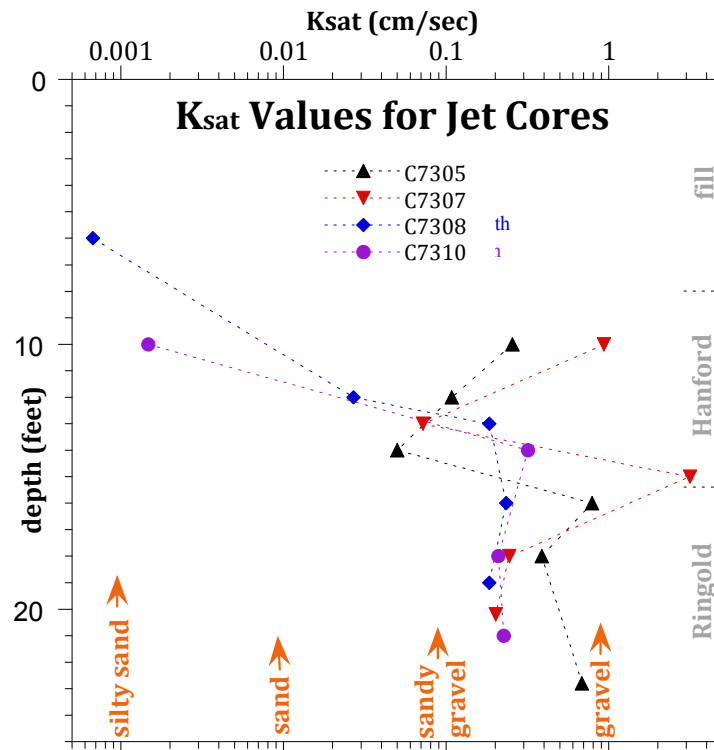


Figure 5.6. Calculated Saturated Hydraulic Conductivity Values for Jet-Injected Cores

In this study, 10 samples were analyzed for total organic carbon (Table 5.2). For borehole N-217, which received only Na-PO_4 jet injection (i.e., no additional organic carbon from the injection), the organic carbon profile with depth (Figure 5.7a, Table 5.3) decreased from 0.2% at 4 ft to 0.16% at 10 ft to 0% at 16 ft. The inorganic carbon content was relatively constant with depth at 0.04% (Figure 5.7b). Jet injection of fish-bone apatite (N-222, red squares in Figure 5.7) doubled the organic carbon at a 6-ft depth where significant apatite was deposited (Figure 5.1b), but resulted in little change at the 11- or 15-ft depth. Jet injection of fish-bone apatite and Na-PO_4 resulted in a three-fold increase in organic carbon (N-219) at an 8-ft depth. In a second borehole (N-220), that did not show much phosphate deposition (Figure 5.2b), the organic carbon content did not increase. The inorganic carbon content of the fish-bone apatite injected boreholes was the same with depth compared to the phosphate-only injection (N-217, Figure 5.7b).

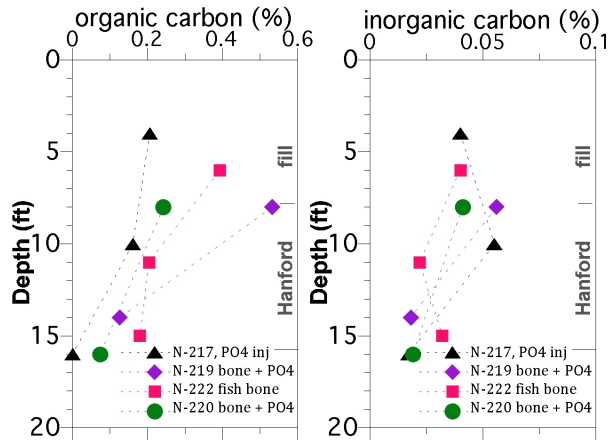


Figure 5.7. Organic Carbon (a) and Inorganic Carbon (b) Depth Profile

Table 5.2. Carbon Analysis of River Samples

injection type	Borehole	depth (ft)	total carbon (%)	inorganic carbon (%)	organic carbon (%)
fish bone apatite	N-222	6.0	0.423 ± 0.065	0.040 ± 0.010	0.392 ± 0.059
		11.0	0.226 ± 0.002	0.022 ± 0.011	0.204 ± 0.002
		15.0	0.211 ± 0.046	0.032 ± 0.009	0.180 ± 0.039
fish bone apatite and Na-PO4	N-220	8.0	0.283 ± 0.014	0.041 ± 0.005	0.242 ± 0.012
		16.0	0.093 ± 0.016	0.019 ± 0.004	0.074 ± 0.013
fish bone apatite and Na-PO4	N-219	8.0	0.588 ± 0.066	0.056 ± 0.005	0.532 ± 0.059
		14.0	0.144 ± 0.024	0.018 ± 0.006	0.126 ± 0.021
Na-PO4	N-217	4.0	0.246 ± 0.028	0.040 ± 0.004	0.206 ± 0.024
		10.0	0.216 ± 0.025	0.055 ± 0.031	0.161 ± 0.019
		16.0	0.018 ± 0.002	0.017 ± 0.005	0.001 ± 0.001

A comparison of the organic matter content to apatite content shows comparable results. Fish-bone apatite is 25% to 45% organic matter, and at a 6-ft depth in the fish-bone injected borehole N-222, organic carbon analysis shows about 0.2% greater organic carbon compared with background organic carbon. This is equivalent to 4 mg/g organic carbon, or an estimated 4 to 8 mg/g PO₄. Phosphate analysis of the sediment (Figure 4.1b) shows 3.2 mg PO₄/g of sediment.

To test the influence of the potential Sr-90 uptake by biomass (i.e., microbes, fungus, etc.), parallel experiments were conducted with 10 g of sediment from two specific depths (C7305, 6-ft depth and C7308, 5.5-ft depth) with and without 240 hours of ultraviolet light treatment. Extractions were conducted to evaluate the difference in Sr-90 adsorbed on the surfaces by ion exchange and by acid extraction (which should remove Sr-90 within biomass). Results showed that some additional Sr-90 was mobilized (i.e., adsorbed to the sediment surface rather than included in biomass) when the biota was subjected to the ultraviolet light treatment (Table 5.3). Unfortunately, the total Sr-90 extracted from the sediment at this jet-injection location is small (Table 5.3, 6-ft depth; also Figures 5.1 through 5.4), as all 60 samples at depth in four boreholes were less than 1 pCi/g Sr-90. Given the standard deviation of counting these low-level samples (± 0.25 pCi/g), two of four samples showed a statistically significant increase in Sr-90 with ultraviolet treatment of two to three times the standard deviation. Therefore, if fish-bone apatite was emplaced in sediment with low Sr-90 concentration, it is likely that uptake of Sr-90

in the biomass and later release (upon biomass death) is not significant. However, if fish-bone apatite was emplaced in sediment with high Sr-90 concentration, the effect could be significant.

Table 5.3. Ultraviolet Light Treatment and Sr-90 Release

borehole	depth (ft)	treatment	Sr-90 ion exch.* (pCi/g)	Sr-90 total* (pCi/g)
N-222	5.5	no UV light	0.14	0.18
N-222	5.5	240 h UV	0.45	0.32
N-219	6.0	no UV light	0.77	0.00
N-219	6.0	240 h UV	0.50	0.86

* ± 0.25 pCi/g

6.0 Summary

6.1 Phosphate and Sr-90 Distribution in River Sediments

Phosphate and ion exchangeable Sr-90 in river sediments near the Ca-citrate-PO₄ injection wells and upriver were analyzed to determine if phosphate injections within the aquifer have influenced Sr-90 retention in river sediments. The upriver sample (N outfall) had 1.8 pCi/g total Sr-90, whereas a river sediment sample (T100N3a) 200 ft northwest of injection well N-138 had 0.66 pCi/g Sr-90. Subsurface sediments near N-138 range from 1 to 23 pCi/g Sr-90. The fraction of ion exchangeable Sr-90 in T100N3a was 7.5% versus 42% for the N outfall sample. The lower ion exchangeable Sr-90 in T100N3a is consistent with the aquifer phosphate treatment, although all values are near detection limits. If the river sediment sample T100N3a is influenced by phosphate precipitate, there should be higher extractable phosphate mass relative to the background (N outfall) sample. Phosphate data did not show elevated levels, with 0.12 mg/g in the T100N3a sample and 0.20 mg/g in the N outfall sample. It should be noted that both samples contain some shells and organic matter, which does contain some phosphate.

6.2 Groundwater Injection of Ca-Citrate-PO₄

The objectives of core analyses used to evaluate the Ca-citrate-PO₄ injections are to characterize a) phosphate mass with depth and radial distance from the injection well(s), and b) Sr-90 distribution adsorbed on sediment and incorporated in apatite. For this location on the downstream end of the 300-ft barrier emplacement, cores from three boreholes (N-368, N-369, and N-370) drilled at different distances from injection well N-137 and adjacent Ringold-only injection well N-159 were characterized. The target apatite concentration (1.7 mg apatite/g of sediment or 0.544 mg PO₄/g) corresponds to a pore volume amendment of 90 mM of phosphate precipitated in sediment with no retardation, or 45 mM phosphate precipitated with a retardation of 2.0 (field observed retardation of 1.6 to 2.4). The 1.7 mg apatite precipitate/g of sediment in the aquifer (20% porosity) will occupy 13.6% of the pore space. Given the 10 mM PO₄ and 40 mM PO₄ injections in 100-N Area wells, an average apatite loading of 1.9 mg apatite/g of sediment (0.608 mg PO₄/g) is expected.

The average phosphate for three boreholes for cores taken in November 2009 (both Hanford formation and Ringold Formation) was 0.415 ± 0.232 mg PO₄/g of sediment, with the Hanford formation average of 0.559 ± 0.253 mg PO₄/g (92% of injected mass) and the Ringold Formation average of 0.268 ± 0.113 mg PO₄/g (44% of injected mass). Phosphate extractions in November 2008 (six borings, along the length of the 300-ft barrier) after just the low concentration Ca-citrate-PO₄ injections (10 mM PO₄) showed 0.150 mg/g in the Hanford formation and 0.041 mg/g in the Ringold Formation. Although these boreholes were located at different distances from the two injection wells, the average phosphate concentration was relatively constant at 0.376 mg/g (N-368), 0.420 mg/g (N-369), and 0.406 mg/g (N-370). This relatively uniform distribution of phosphate with radial distance from the point of injection demonstrates one benefit of the Ca-citrate-PO₄ amendment groundwater injection; namely that the solution can be injected without precipitation occurring for tens of hours (50 to 200 hours citrate biodegradation half-life).

Within both the Hanford formation and Ringold Formation, there is spatial variability of the measured PO₄ concentration with depth (Figure 4.2 through 4.4). In most cases, high phosphate at a given depth

corresponds to high total Sr-90 values. It is hypothesized that this correlation between PO_4 and Sr-90 concentration is related to finer grained sediment zone with higher surface area (and more ion exchange sites). Borehole N-370 is 15.7 ft from fully screened injection well N-137 and 9.5 ft from Ringold-only screened well N-159. Analysis of the N-370 cores showed similar phosphate mass in the Ringold formation as was observed at the other two borehole locations, but elevated phosphate in the Hanford formation (0.72 mg/g). This higher phosphate mass is likely associated with overlap with the Hanford formation treatment in the adjacent injection well (N-136), which was injected during relatively low river stage conditions that resulted in a larger radial extent of treatment than planned (see Vermeul et al. 2010, Figure A.11).

A sediment sample from borehole N-368, 12-ft depth was analyzed using an EDS detector on a SEM to identify surface phosphate precipitate crystal structure. Phosphate precipitates occur in small less than 50-micron conglomerates of finer grained precipitate at a low concentration. Apatite crystal structure was previously identified in precipitate in sediment in a laboratory experiment with the Ca-citrate- PO_4 solution (Szecsody et al. 2009). For these field sediments, 17 of 36 locations examined by SEM/EDS did show phosphorous in a crystal structure, but the apatite crystal structure was not positively identified.

Sr-90 (and Sr) behaves nearly the same as calcium in the Hanford Site 100-N Area sediments, so is found primarily adsorbed by ion exchange to sediments. The ion exchangeable Sr-90 (triangles, Figures 4.2 through 4.4) are 50.6% of the total Sr-90 in zones of PO_4 treatment in the Hanford formation and Ringold Formation. With pre-injection conditions of 90% ion exchangeable Sr-90, the data indicates 39.4% Sr-90 was incorporation into apatite by 1 year. It is expected that additional Sr-90 will be incorporated into apatite in the following years, because Sr-apatite is thermodynamically more stable than Ca-apatite (Verbeek et al. 1977). Laboratory experiments conducted over 1.3 years do show a continued uptake of strontium (Szecsody et al. 2009). Ion exchange flushing due to the Ca-citrate- PO_4 solution injection also accounts for low Sr-90 values in the injection zone. It is estimated that 47% of the Sr-90 was flushed out of the injection zone into nearby sediments during injection, based on pre- and post-injection ion exchangeable calcium in the sediment. Background (natural) ion exchange conditions of calcium and strontium (and Sr-90) are expected to be reestablished within a few years. Therefore, within the next few years to decades, Sr-90 aqueous values are expected to rise (from reestablishment of equilibrium conditions) and then fall as additional Sr-90 is incorporated into apatite.

The grain-size distributions and calculated saturated hydraulic conductivities for boreholes N-368 and N-370 (Figures 4.2 through 4.4) show relatively even distributions with depth, and N-369 shows a fine-grained zone at an 18-ft depth. There is a general correlation of finer grained sediment (i.e., more sorption with higher surface area) with elevated Sr-90 and PO_4 . The total Sr-90 and extracted PO_4 data show good correlation ($R = 0.82$). It should be noted that over time (decades) the apatite accumulates Sr-90 in the structure, so this correlation will become stronger as upgradient Sr-90 flows into the apatite-laden zone.

6.3 Jet-Injected Phosphate and Apatite

This task was initiated to evaluate the mass of phosphate with depth for four locations that were jet injected with combinations of sodium phosphate and solid apatite (i.e., “Apatite II” or fish-bone apatite). Additional analysis was conducted on the cores, which includes a) total Sr-90 and ion exchangeable Sr-90, b) ion exchangeable calcium and strontium, c) grain-size distributions and calculated saturated

hydraulic conductivity, and d) TOC. TOC analyses have not been completed. Borehole N-217, which was water jetted with sodium phosphate only, had an average of 1.2 mg PO₄/g of sediment, whereas N-222 (water jetted with fish bone only) had an average of 1.63 mg PO₄/g. The two other boreholes (N-219 and N-220), in which both sodium phosphate and fish-bone apatite was water jetted, had an average of 1.76 mg PO₄/g. The target apatite content of 1.7 mg apatite/g of sediment corresponds to 0.54 mg PO₄/g of sediment. The 1.7 mg apatite precipitate/g of sediment in the aquifer (20% porosity) will occupy 13.6% of the pore space, so a much greater mass of phosphate precipitate can lead to decreased permeability. Because jet injections are likely altering the pore space, it is not clear what fraction of pore space high precipitate mass occupies. From the phosphate mass alone, there was little difference between injected phosphate sources.

The vertical variability in phosphate content in the four jet-injection boreholes was considerable, with a standard deviation nearly equal to the average (Table 4.1). In contrast, water-injected boreholes near N-137 (N-368, N-369, and N-370) standard deviation was about half of the average. Phosphate mass variability could be caused by formation properties (i.e., jetting in finer, looser sediment may cause liquefaction compared with coarser sediments) and/or jetting operations (i.e., ponding phosphate liquid in shallow trenches at the surface). Two boreholes (N-219 and N-217) did show high phosphate in shallow (less than 10 ft) sediment. Borehole N-222 also showed a phosphate spike at the 21-ft depth. All of these high phosphate depths were finer grained sediment (based on the fraction less than 4 mm, and K_{sat} value), and indirect evidence of higher ion exchangeable calcium, strontium, and Sr-90. Therefore, jet injections appear to have emplaced greater phosphate in finer grained zones. Ponding of phosphate liquid at the surface may also have contributed to some of the phosphate observed (boreholes N-217 and N-219), but elevated phosphate was not observed in shallow (coarse grained) sediments in boreholes N-220 and N-222, so infiltration of ponded water could not explain the observed phosphate profiles.

Sr-90 values in all four boreholes (Figures 4.1a through 4.4a) are all less than 5 pCi/g (total Sr-90), so considerably lower than the 90-pCi/g peak at a 15-ft depth in N-123, which is 230 ft to the northeast of N-222. Mobile Sr-90 is either aqueous or on ion exchange surfaces. Once Sr-90 is incorporated into apatite, it is considerably less mobile (i.e., dependent on the dissolution of the low solubility apatite). The fraction of ion exchangeable Sr-90 did vary with injected phosphate source, with N-217 (phosphate injection) at $0.12 \pm 0.11\%$, with N-222 (fish-bone injection) at $0.20 \pm 0.12\%$, and N-219 and N-220 (fish-bone and apatite injection) at $0.19 \pm 0.16\%$ and $0.23 \pm 0.12\%$, respectively. Greater Sr-90 incorporation into field-formed phosphate precipitates (with the phosphate only injection) likely resulted in lower fraction of ion exchangeable Sr-90 for the phosphate only injections.

Therefore, high pressure water jetting is a viable technology to emplace phosphate or apatite in subsurface sediments. It does appear to emplace higher PO₄ mass in finer grained sediments compared with Ca-citrate-PO₄ groundwater injections (reported in this study) or Ca-citrate-PO₄ solution infiltration (Szecsody et al. 2009). The spatial variability of the emplaced phosphate mass is greater (81% standard deviation) than water-saturated zone injected Ca-citrate-PO₄ (43% standard deviation). Jet injection of phosphate only resulted in a greater fraction of Sr-90 incorporated into phosphate precipitates at the time of this core sampling. Over time, depths that received solid-phase apatite mass will also incorporate additional Sr-90 mass into the apatite. The fish-bone apatite injected (cores N-219, N-220, and N-222) contains 25% to 45% organic matter. Organic carbon measured in 10 sediment samples did show an increase as high as 0.2% (grams of organic carbon per gram of sediment) over natural organic carbon. Because biomass will grow on this organic matter (and the supplied phosphate source), there is some uptake of Sr-90. Subsequent death of the biomass when the organic matter is depleted can lead to Sr-90

release. Experiments conducted to assess Sr-90 release upon biomass death did show an increase in ion exchangeable Sr-90. However, because the total Sr-90 in the samples used was low (less than 1 pCi/g), the release was insignificant.

6.4 Comparison of Groundwater and Jet Injections

The purpose of phosphate addition to 100-N Area subsurface sediments (as an aqueous chemical or precipitate) is to adsorb and eventually incorporate Sr-90 as a permeable reactive barrier during groundwater flow of Sr-90 toward the Columbia River. Approximately 1.7 mg of apatite/g of sediment is needed (equivalent to 0.54 mg PO₄/g sediment) to remove strontium (and Sr-90) from solution for 300 years (10 half-lives of Sr-90 decay), assuming 10% substitution of strontium for calcium in the apatite structure. Greater apatite mass will result in more complete Sr-90 removal, even during high groundwater flow events, whereas less apatite mass will result in some Sr-90 breakthrough. Sr-90 contamination varies spatially, but 40% to 70% of the mass is in the variably saturated zone of the Hanford formation with less contamination in the underlying Ringold Formation. Groundwater injections of Ca-citrate-PO₄ into all of the Hanford formation is difficult, and requires injections seasonally timed at high river stage (and high groundwater level in the unconfined aquifer). Therefore, alternate strategies such as Ca-citrate-PO₄ solution infiltration and jet injection of phosphate mass are being investigated to emplace mass in the Hanford formation.

Jet injection of fish-bone apatite and sodium phosphate in shallow (less than the 16-ft depth) 100-N Area sediments show high phosphate concentrations (0.80 to 2.7 mg/g), as evidenced by phosphate extractions from sediments at 1.0, 2.5, and 3.8 ft from the nearest jet-injection point (with additional nearby injection points; Table 6.1). The jet-injected phosphate mass was also highly variable spatially, as evidenced by the PO₄ average in two boreholes (N-220 and N-219) near PO₄/apatite injections being three times different (i.e., 0.8 mg/g and 2.7 mg/g). In addition, three of four injected boreholes show high phosphate correlated with finer grained sediment zones. Therefore, while jet injection of multiple phosphate sources in all cases exceeded the calculated 0.54 mg PO₄/g of sediment, the data also shows a significant decrease in PO₄ mass with distance from the injection point (data only at 1.0, 2.5, and 3.8 ft radial distance from injections; Figure 6.1), and the spatial variability (averaging 81% of the mean value) is significant. High phosphate mass can also lead to a decrease in permeability (as described earlier), although it is unclear how much pore space the precipitate is occupying for jet injections as the system is likely physically altered by liquifaction (fine grained sediments) or fractures. In contrast, groundwater injection of a Ca-citrate-PO₄ solution appears to result in a more even phosphate distribution radially from injection wells (6.5, 10.0, and 15.7 ft; Table 6.1), with average PO₄ in the Ringold Formation of 0.28, 0.30, and 0.27 mg/g and in the Hanford formation of 0.51, 0.50, and 0.72 mg/g. The spatial variability of the phosphate mass was half that of jet injections, averaging 43% of the mean value.

It is, however, not possible to compare technical merits of Ca-citrate-PO₄ solution to jet-injected phosphate in terms of mass delivered to the subsurface data for the two different technologies at different distances from the injected source. Phosphate data for jet injections is only available at 1.0 to 3.8 ft from the nearest injection point, whereas phosphate data is available for Ca-citrate-PO₄ injections at 6.5 to 15.7 ft from the nearest injection. The closest comparison that can be made is jet injections deposited 0.54 mg/g PO₄ at a 3.8-ft distance from injections whereas groundwater injection of Ca-citrate-PO₄ deposited 0.37 to 0.42 mg/g PO₄ at 6.45- to 15.7-ft distance from injections. In addition to a comparison

of the spatial distribution of phosphate deposition, a comparison should also be made of the relative cost of phosphate emplacement by the two technologies.

Table 6.1. Phosphate Content in All Boreholes

borehole	injection	average PO ₄ * (mg/g)	fill PO ₄ * (mg/g)	Hanford Fm PO ₄ * (mg/g)	Ringold Fm PO ₄ * (mg/g)	distance to PO ₄ injection (ft)	distance to additional PO ₄ injection wells (ft)
jet injection of apatite and/or Na-PO₄							
N-222	apatite	1.63 ± 1.35	1.14 ± 1.04	1.81 ± 1.14	1.82 ± 1.91	0.99	5.1,5.3,5.8,6.0,8.4
N-220	PO ₄ , apatite	0.80 ± 0.48	1.39 ± 0.19	0.39 ± 0.30	0.40 ± 0.36	3.78	4.19, 7.57
N-219	PO ₄ , apatite	2.73 ± 2.99	5.90 ± 4.19	2.06 ± 1.41	1.00 ± 1.07	2.51	5.82, 7.44
N-217	PO ₄	1.20 ± 1.96	2.58 ± 3.55	0.89 ± 0.98	0.45 ± 0.13	1.06	3.7,5.2,6.4,9.1,11.4
groundwater injection of Ca-citrate-PO₄							
N-368	Ca-citrate-PO ₄	0.376 ± 0.180	0.092±0.155	0.510±0.138	0.276±0.099	6.5	23.0
N-369	Ca-citrate-PO ₄	0.420 ± 0.147	0.365±0.126	0.497±0.056	0.305±0.189	10.0	17.0
N-370	Ca-citrate-PO ₄	0.406 ± 0.346	0.193±0.085	0.719±0.518	0.269±0.128	15.7	9.5

* using average background PO₄ = 0.46 mg/g

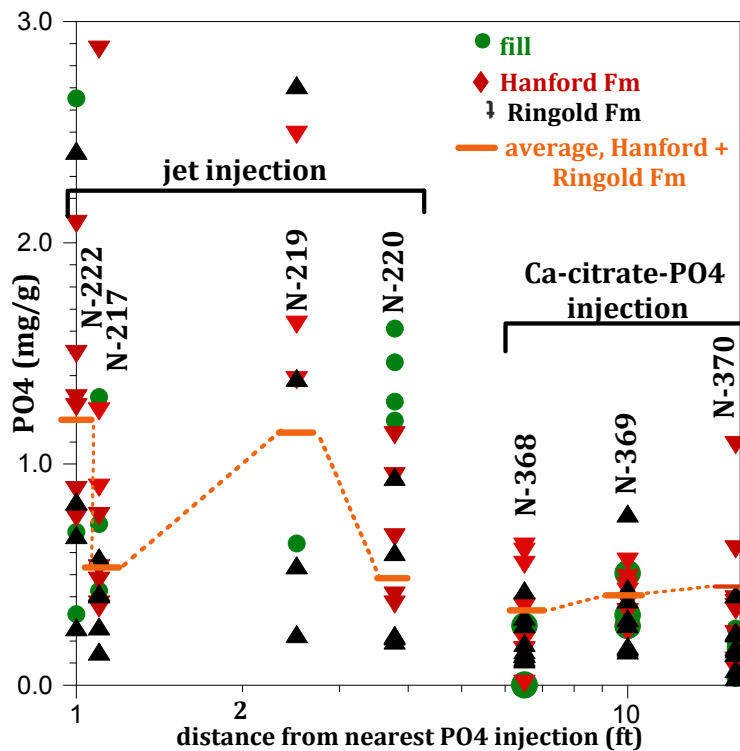


Figure 6.1. Phosphate Content and Distance from Injection (all boreholes)

Overall, both technologies (groundwater injection of Ca-citrate-PO₄) and water-jet injection of sodium phosphate/fish-bone apatite) delivered sufficient phosphate to subsurface sediments in the 100-N Area to be effective in adsorbing and then incorporating Sr-90 into the apatite structure. The Ca-citrate-PO₄ injection technology is better established, with a significant number of laboratory- and field-scale

injection tests. This technology delivers a fairly even distribution of phosphate to subsurface sediments because the solution is stable for tens of hours before Ca-PO₄ precipitation occurs, allowing time to inject. The even distribution of phosphate is limited by formation heterogeneities and ability to inject into the formation. As described in Vermeul et al. (2010), both this core analysis and aqueous breakthrough data during injections showed that target PO₄ concentrations were generally met or exceeded within the saturated portion of the Hanford formation, while Ringold Formation wells were generally at or below the established performance metric of 20% to 30% concentration at a radial distance of 30 ft (i.e., at adjacent injection wells). Groundwater injections of Ca-citrate-PO₄ into the upper portion of the Hanford formation requires injections timed only at high river stage, which reduces the time period available for injection. Alternate strategies such as Ca-citrate-PO₄ solution infiltration and jet injection of phosphate mass are being investigated to emplace mass in the shallow Hanford formation. Jet injection of sodium phosphate, fish-bone apatite, and a combination of both did deliver significant phosphate to the Hanford formation (i.e., 8 to approximately 15 ft depth), but the data was taken very close to injection points (1 ft, 2.5 ft, and 3.8 ft; Table 6.1), so it is difficult to assess the relevant areal extent (i.e., 5 to 20 ft) and injection point spacing that should be used. Jet injections used by others to emplace zero valent iron at other sites qualitatively indicate 10-ft spacing between injection points is sufficient. In addition, jet injection appears to deposit more phosphate in finer grained sediments, so the spatial variability of the phosphate mass is much greater (standard deviation was 81% of the mean phosphate mass) than Ca-citrate-PO₄ injections (43% of the mean). A mechanism that could explain these results is finer grained sediments (and colloids) are mobilized, which results in more complete mixing of the phosphate in the sediment, whereas dendritic fracture patterns may develop with phosphate jetting into coarser grained sediments. This may also cause some change in the sediment hydraulic conductivity. This jet injection technology is new to the Hanford Site 100-N Area, so further testing is needed to quantify limitations and causes of these effects.

7.0 References

- Bellin CA and PSC Rao. 1993. "Impact of Bacterial Biomass on Contaminant Sorption and Transport in a Subsurface Soil." *Applied and Environmental Microbiology* 59(6), 1813–1820.
- Chairat C, EH Oelkers, S Kohler, N Harouiya, and JE Lartique. 2004. "An Experimental Study of the Dissolution Rates of Apatite and Britholite as a Function of Solution Composition and pH from 1-12." In *Water-Rock Interaction*, WS White II (ed.), pp. 671–674. Taylor & Francis Group, London.
- Folk R. 1974. *Petrology of Sedimentary Rocks*. Hemphill Publishing Company, Austin, Texas.
- Heslop DD, Y Bi, AA Baig, M Otsuka, and WI Higuchi. 2005. "A Comparative Study of the Metastable Equilibrium Solubility Behavior of High-Crystallinity and Low-Crystallinity Carbonated Apatites Using pH and Solution Strontium as Independent Variables." *Journal of Colloid and Interface Science* 289:14–25.
- Lazic S and Z Vukovic. 1991. "Ion-Exchange of Strontium on Synthetic Hydroxyapatite." *Journal of Radioanalytical and Nuclear Chemistry-Articles* 149:161–168.
- LeGeros RZ, G Quiroigico, and JP LeGeros. 1979. "Incorporation of Strontium in Apatite - Effect of pH." *Journal of Dental Research* 58:169–179.
- Masch FD and KJ Denny. 1966. "Grain Size Distribution and its Effect on the Permeability of Unconsolidated Sands." *Water Resour. Res.* 2(4):665–677.
- McKinley JP, JM Zachara, SC Smith, and C Liu. 2007. "Cation Exchange Reactions Controlling Desorption of $^{90}\text{Sr}^{2+}$ from Coarse-Grained Contaminated Sediments at the Hanford Site, Washington." *Geochimica et Cosmochimica Acta* 71(2):305–325.
- Moore RC, C Sanchez, K Holt, P Zhang, H Xu, and GR Choppin. 2004. "Formation of Hydroxyapatite in Soils Using Calcium Citrate and Sodium Phosphate for Control of Strontium Migration." *Radiochimica Acta* 92(9-11/2004):719–723.
- Moore R, J Szecsody, M Truex, K Kelean, R Bontchev, and C Ainsworth. 2007. "Formation of Nanosize Apatite Crystals in Sediments for Contaminant and Stabilization of Contaminants." *Environmental Applications of Nanomaterials, Synthesis, Sorbents, and Sensors*, (eds) G Fryxell and G Cao, Imperial College Press, pp. 89–109.
- Raicevic S, Z Vukovic, TL Lizunova, and VF Komarov. 1996. "The Uptake of Strontium by Calcium Phosphate Phase Formed at an Elevated pH." *Journal of Radioanalytical and Nuclear Chemistry-Articles* 204:363–370.
- Serne RJ and VL LeGore. 1996. *Strontium-90 Adsorption-Desorption Properties and Sediment Characterization at the 100-N Area*. Pacific Northwest Laboratory, Richland, Washington.
- Steeffel CI. 2004. "Evaluation of the Field-Scale Cation Exchange Capacity of Hanford Sediments." In *Water-Rock Interaction*, WS White II (ed.), pp. 999–1002, Taylor & Francis Group, London.

Szecsody J, C Burns, R Moore, J Fruchter, V Vermeul, D Girvin, J Phillips, and M Williams. 2007. Hanford 100N Area Apatite Emplacement: Laboratory Results of Ca-Citrate-PO₄ Solution Injection and Sr-90 Immobilization in 100N Sediments. PNNL-16891, Pacific Northwest National Laboratory, Richland, Washington.

Szecsody J, M Rockhold, M Oostrom, R Moore, C Burns, M Williams, L Zhong, J Fruchter, J McKinley, V Vermeul, M Covert, T Wietsma, A Breshears, and B Garcia. 2009. *Sequestration of Sr-90 Subsurface Contamination in the Hanford 100-N Area by Surface Infiltration of a Ca-Citrate-Phosphate Solution*. PNNL-18303, Pacific Northwest National Laboratory, Richland, Washington.

Verbeek RMH, M Hauben, HP Thun, and F Verbeek. 1977. "Solubility and Solution Behavior of Strontium Hydroxyapatite." *Z. Phys. Chem. (Wiesbaden)* 108(2):203–215.

Vermeul VR, JE Szecsody, BG Fritz, MD Williams, and JS Fruchter. 2010. *100-NR-2 Apatite Treatability Test F09 Status: High-Concentration Calcium-Citrate-Phosphate Solution Injection for In Situ Strontium-90 Immobilization, Final Report*. PNNL report, in press, Pacific Northwest National Laboratory, Richland, Washington, 138 pp.

Williams M, B Fritz, D Mendoza, M Rockhold, P Thorne, Y Xie, B Bjornstad, R Mackley, D Newcomer, J Szecsody, and V Vermeul. 2008. *Interim Report: 100-NR-2 Apatite Treatability Test: Low-Concentration Calcium-Citrate-Phosphate Solution Injection for In Situ Strontium-90 Immobilization*. PNNL-17429, Pacific Northwest National Laboratory, Richland, Washington.

Wright J, KR Rice, B Murphy, and J Conca. 2004. "PIMS Using Apatite II™: How It Works To Remediate Soil and Water." *Sustainable Range Management*, RE Hinchee and B Alleman (eds.), Battelle Press, Columbus, Ohio. www.batelle.org/bookstore, ISBN 1-57477-144-2, B4-05.

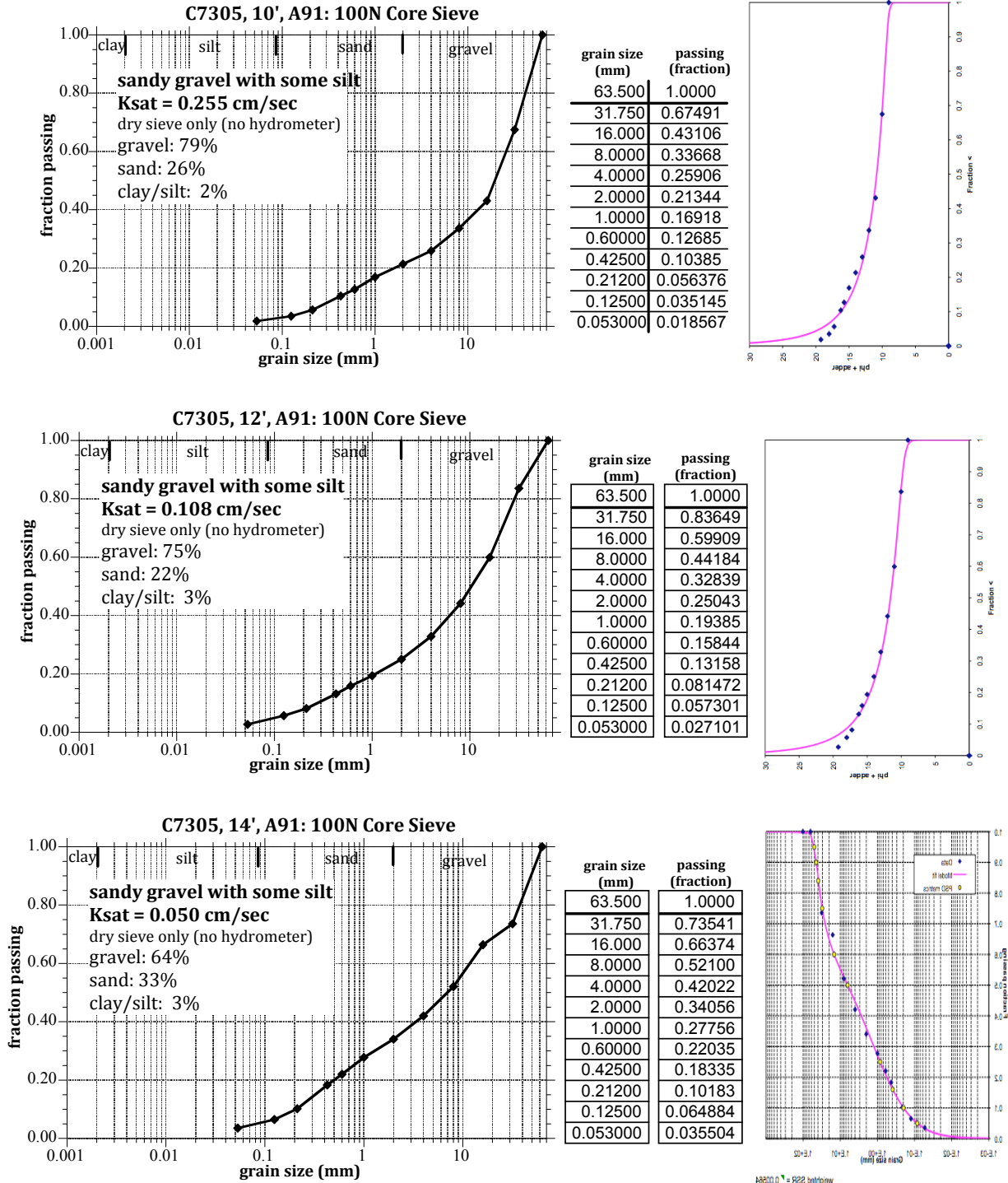
Appendix A

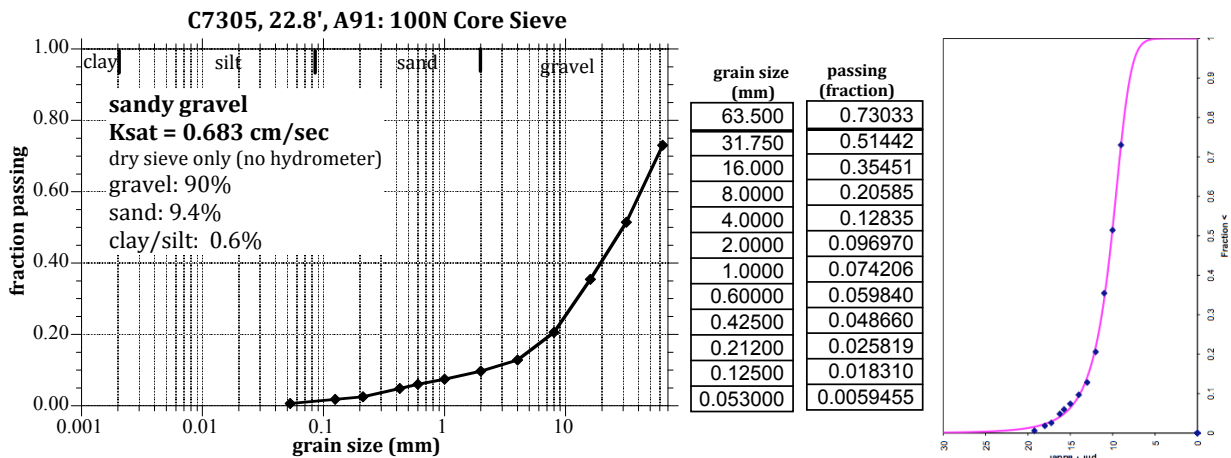
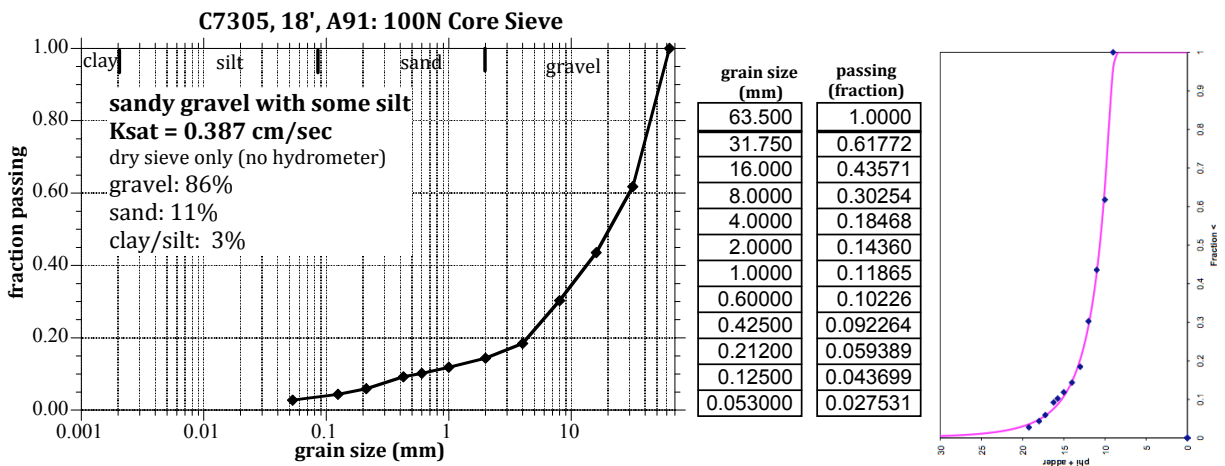
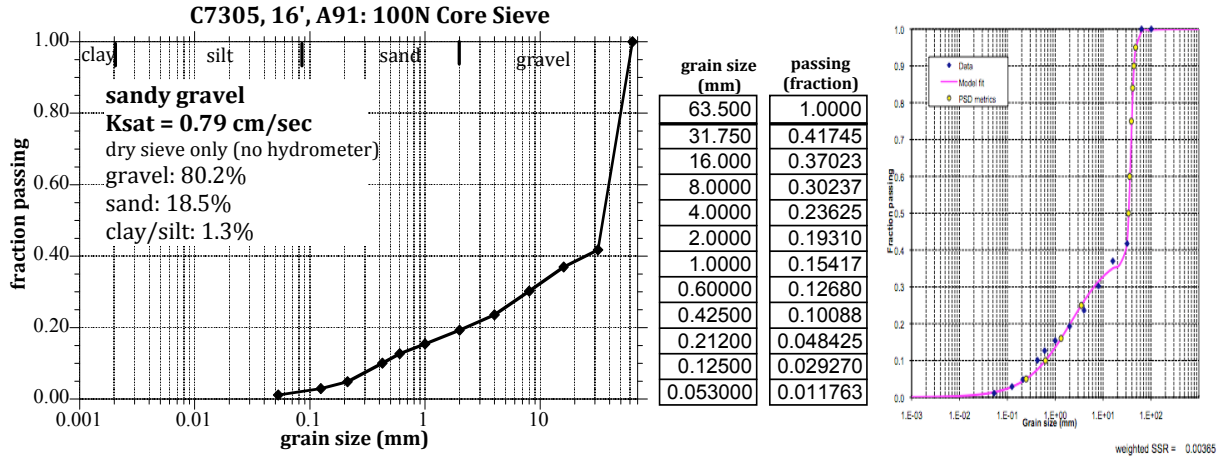
Jet-Injection Grain-Size Distributions

Appendix A

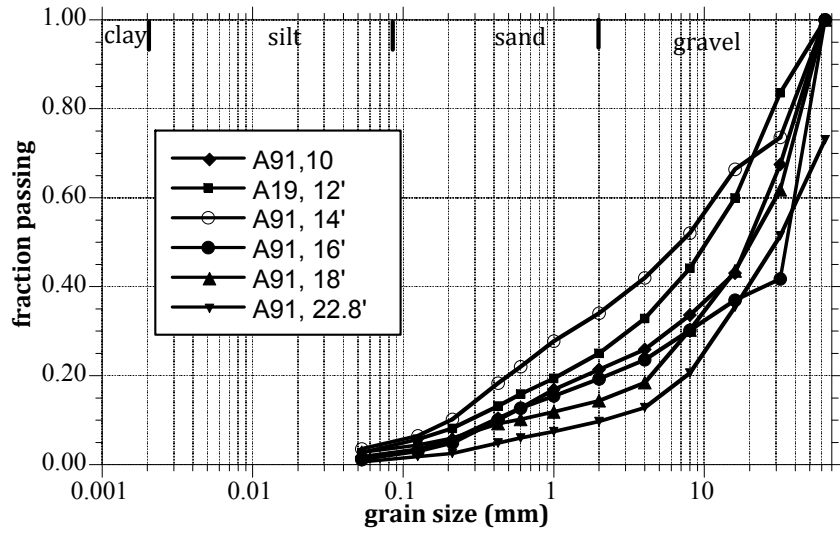
Jet-Injection Grain-Size Distributions

Purple line fit to grain-size data (graph at right) is described in Section 3.2.

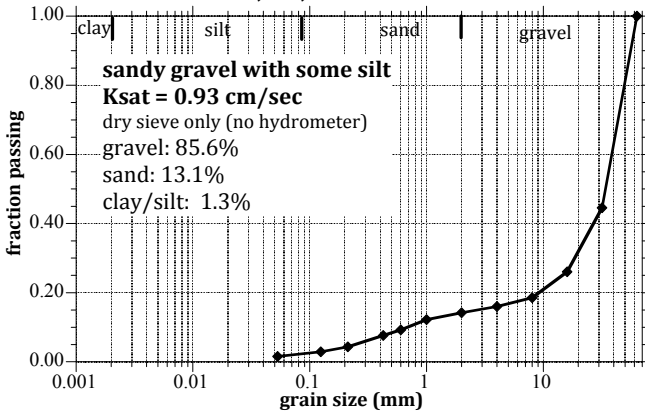




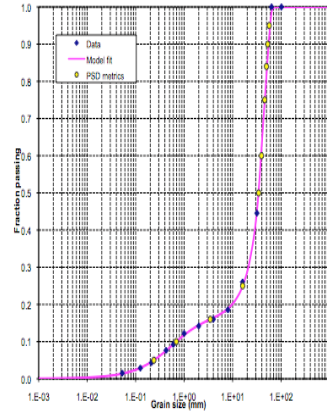
C7305, all depths, A91: 100N Core Sieve



C7307, 10', A92: 100N Core Sieve

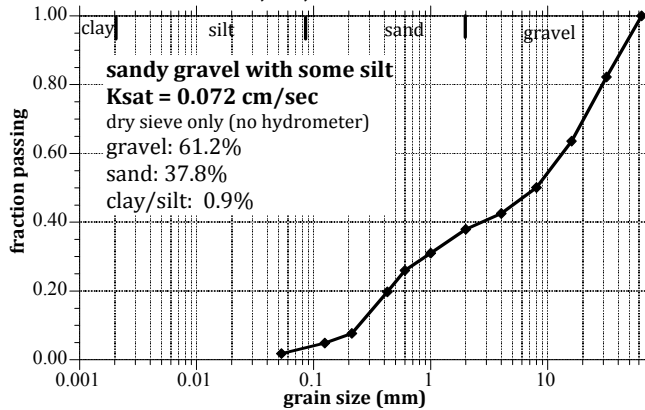


grain size (mm)	passing (fraction)
63.500	1.0000
31.750	0.44555
16.000	0.26029
8.0000	0.18540
4.0000	0.16024
2.0000	0.14189
1.0000	0.12212
0.60000	0.092393
0.42500	0.076336
0.21200	0.043267
0.12500	0.028797
0.053000	0.015392

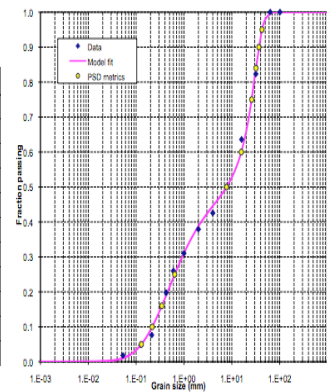


weighted SSR = 0.00038

C7307, 13', A92: 100N Core Sieve

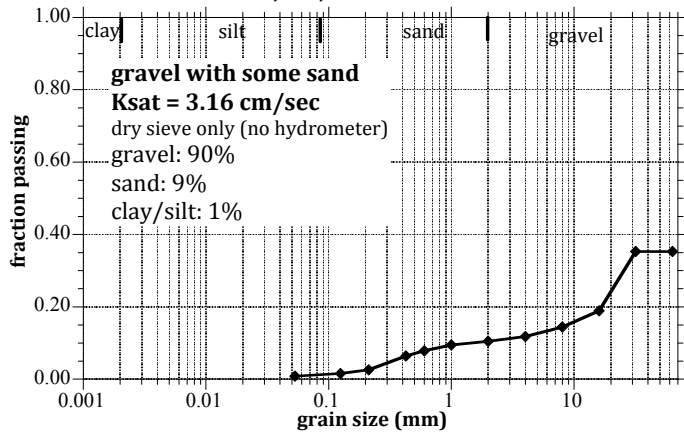


grain size (mm)	passing (fraction)
63.500	1.0000
31.750	0.82297
16.000	0.63600
8.0000	0.50050
4.0000	0.42574
2.0000	0.37937
1.0000	0.31039
0.60000	0.25986
0.42500	0.19761
0.21200	0.076601
0.12500	0.048472
0.053000	0.018441

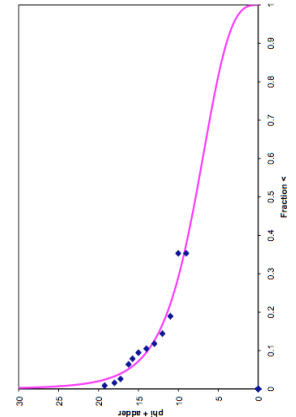


weighted SSR = 0.00270

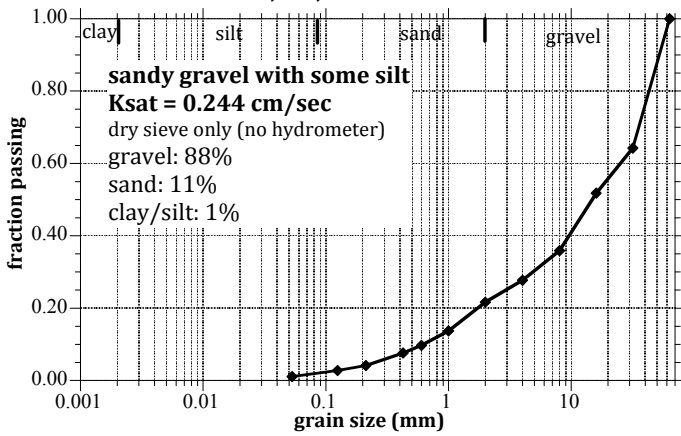
C7307, 15', A92: 100N Core Sieve



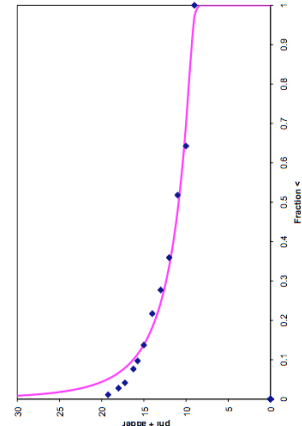
grain size (mm)	passing (fraction)
63.500	0.35317
31.750	0.35317
16.000	0.18924
8.0000	0.14415
4.0000	0.11790
2.0000	0.10486
1.0000	0.094430
0.60000	0.078635
0.42500	0.064180
0.21200	0.026067
0.12500	0.015891
0.053000	0.0086896



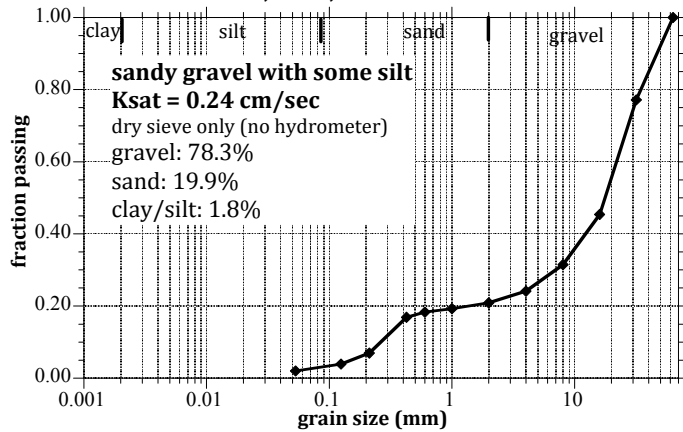
C7307, 18', A92: 100N Core Sieve



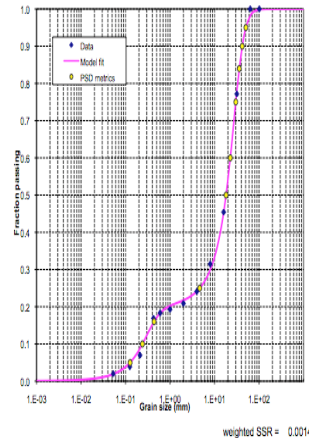
grain size (mm)	passing (fraction)
63.500	1.0000
31.750	0.64274
16.000	0.51804
8.0000	0.35928
4.0000	0.27710
2.0000	0.21708
1.0000	0.13716
0.60000	0.097012
0.42500	0.076455
0.21200	0.041429
0.12500	0.027832
0.053000	0.011113



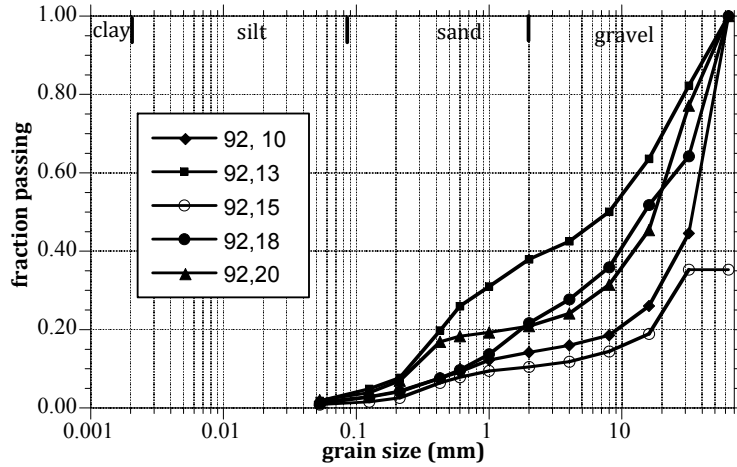
C7307, 20.2', A92: 100N Core Sieve



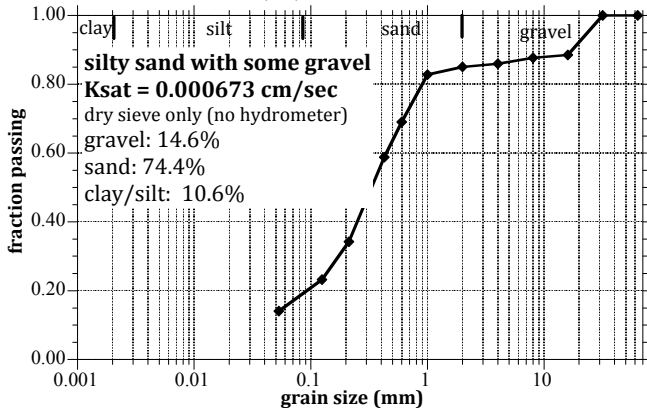
grain size (mm)	passing (fraction)
63.500	1.0000
31.750	0.77150
16.000	0.45423
8.0000	0.31463
4.0000	0.24118
2.0000	0.20899
1.0000	0.19280
0.60000	0.18328
0.42500	0.16912
0.21200	0.069643
0.12500	0.038913
0.053000	0.019835



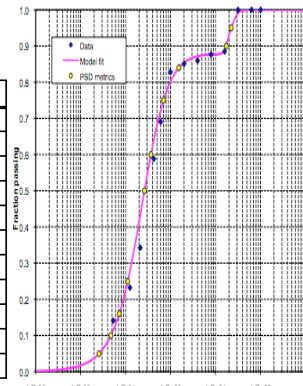
C7307, all depths, A92: 100N Core Sieve



C7308, 6', A93: 100N Core Sieve

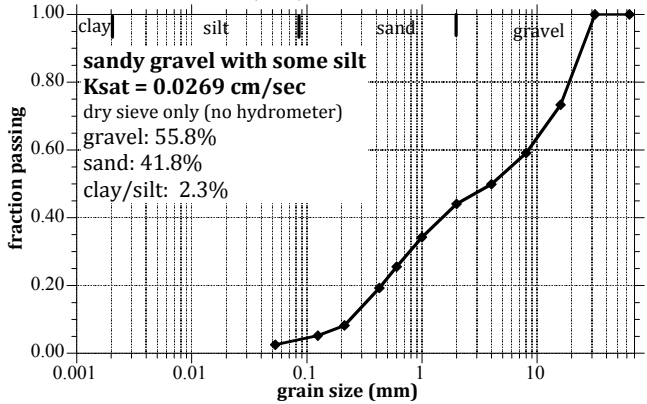


grain size (mm)	passing (fraction)
63.500	1.0000
31.750	1.0000
16.000	0.88520
8.0000	0.87681
4.0000	0.85957
2.0000	0.85085
1.0000	0.82811
0.60000	0.69048
0.42500	0.58824
0.21200	0.34243
0.12500	0.23239
0.053000	0.14086

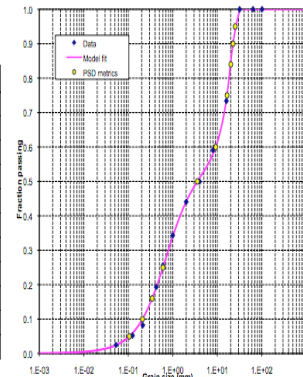


weighted SSR = 0.02998

C7308, 12', A93: 100N Core Sieve

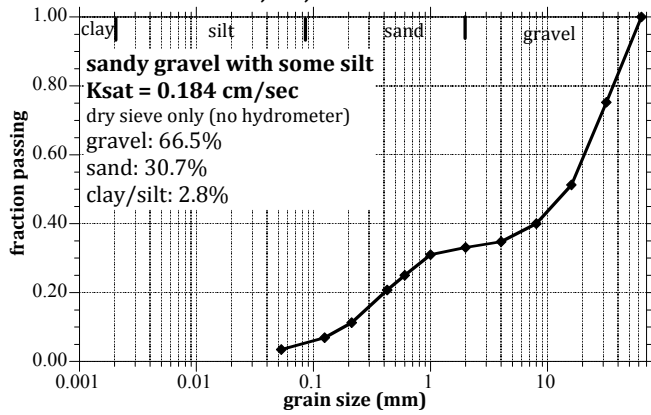


grain size (mm)	passing (fraction)
63.500	1.0000
31.750	1.0000
16.000	0.73375
8.0000	0.59100
4.0000	0.49926
2.0000	0.44075
1.0000	0.34303
0.60000	0.25569
0.42500	0.19329
0.21200	0.082124
0.12500	0.052422
0.053000	0.025107

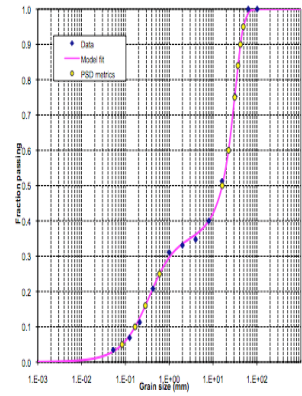


weighted SSR = 0.00079

C7308, 13', A93: 100N Core Sieve

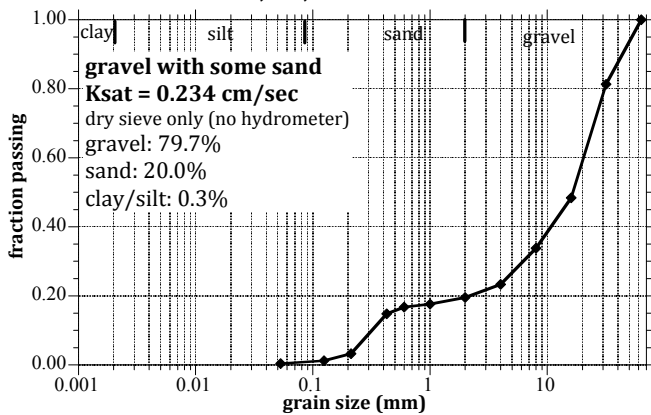


grain size (mm)	passing (fraction)
63.500	1.0000
31.750	0.75310
16.000	0.51256
8.0000	0.40017
4.0000	0.34755
2.0000	0.33096
1.0000	0.31041
0.60000	0.25012
0.42500	0.20790
0.21200	0.11284
0.12500	0.069073
0.053000	0.034586

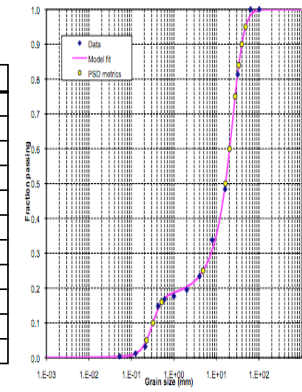


weighted SSR = 0.0018

C7308, 16', A93: 100N Core Sieve

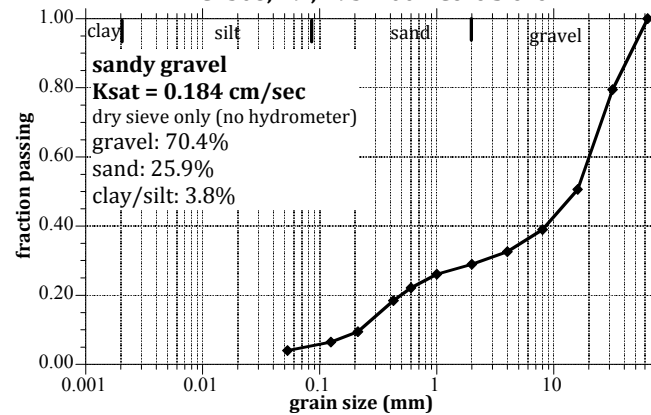


grain size (mm)	passing (fraction)
63.500	1.0000
31.750	0.81336
16.000	0.48408
8.0000	0.33803
4.0000	0.23385
2.0000	0.19516
1.0000	0.17651
0.60000	0.16790
0.42500	0.14803
0.21200	0.032285
0.12500	0.012220
0.053000	0.0034307

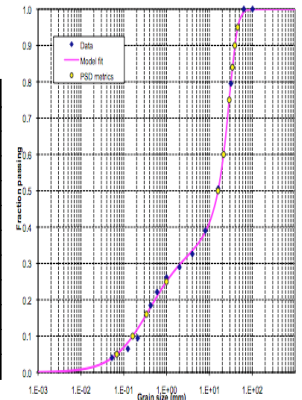


weighted SSR = 0.0016

C7308, 19', A93: 100N Core Sieve

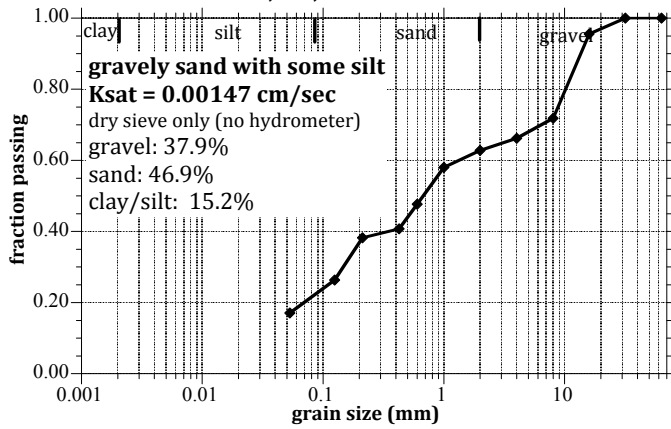


grain size (mm)	passing (fraction)
63.500	1.0000
31.750	0.79503
16.000	0.50620
8.0000	0.39022
4.0000	0.32597
2.0000	0.28965
1.0000	0.26114
0.60000	0.22135
0.42500	0.18442
0.21200	0.094740
0.12500	0.065012
0.053000	0.040202

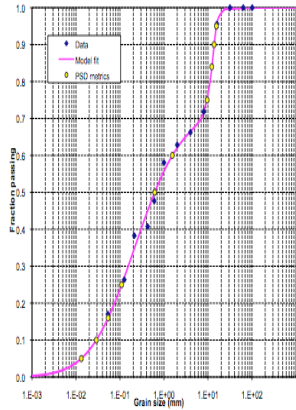


weighted SSR = 0.0014

C7310, 10', A94: 100N Core Sieve

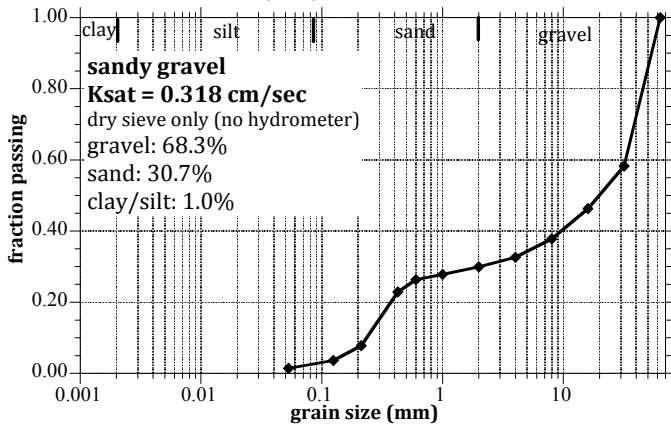


grain size (mm)	passing (fraction)
63.500	1.0000
31.750	1.0000
16.000	0.95614
8.0000	0.71848
4.0000	0.66242
2.0000	0.62845
1.0000	0.58045
0.60000	0.47672
0.42500	0.40742
0.21200	0.38276
0.12500	0.26342
0.053000	0.17034

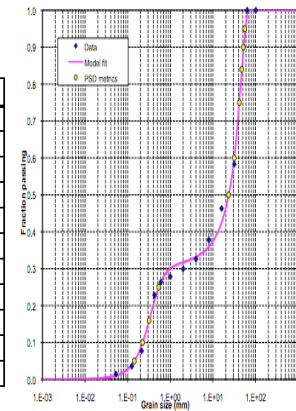


weighted SSR = 0.00425

C7310, 14', A94: 100N Core Sieve

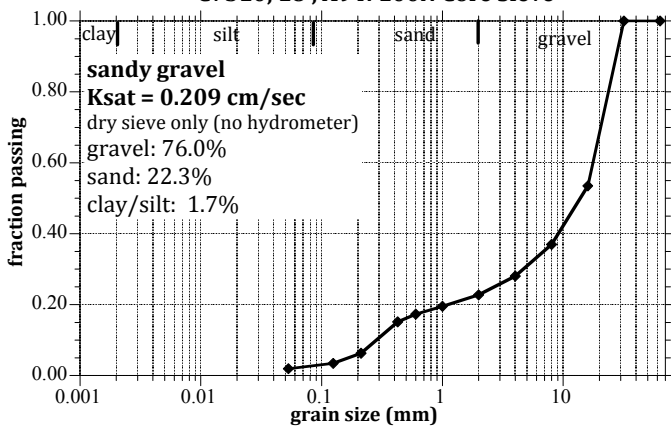


grain size (mm)	passing (fraction)
63.500	1.0000
31.750	0.58287
16.000	0.46323
8.0000	0.37817
4.0000	0.32612
2.0000	0.29950
1.0000	0.27838
0.60000	0.26355
0.42500	0.22879
0.21200	0.077373
0.12500	0.035890
0.053000	0.014347

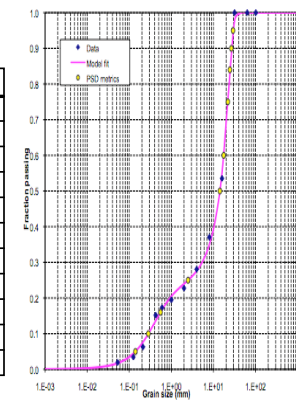


weighted SSR = 0.00377

C7310, 18', A94: 100N Core Sieve

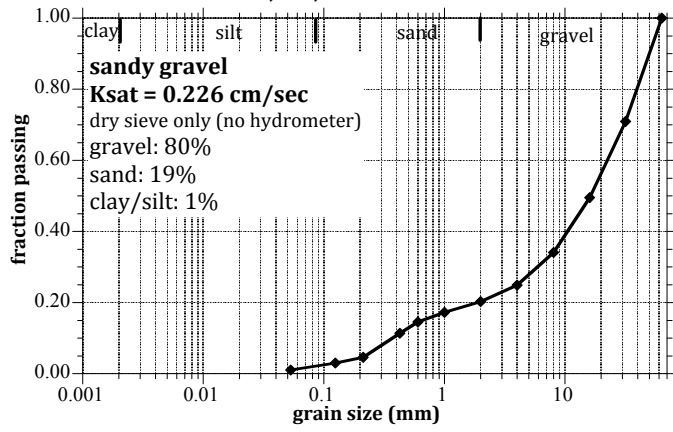


grain size (mm)	passing (fraction)
63.500	1.0000
31.750	1.0000
16.000	0.53529
8.0000	0.37030
4.0000	0.28084
2.0000	0.22744
1.0000	0.19476
0.60000	0.17273
0.42500	0.15165
0.21200	0.062680
0.12500	0.034374
0.053000	0.019354

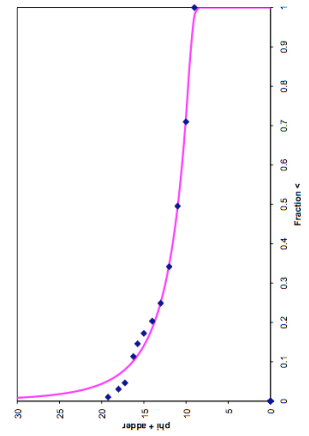


weighted SSR = 0.00203

C7310, 21', A94: 100N Core Sieve



grain size (mm)	passing (fraction)
63.500	1.0000
31.750	0.70984
16.000	0.49562
8.0000	0.34161
4.0000	0.24888
2.0000	0.20327
1.0000	0.17227
0.60000	0.14582
0.42500	0.11342
0.21200	0.046302
0.12500	0.030558
0.053000	0.010232

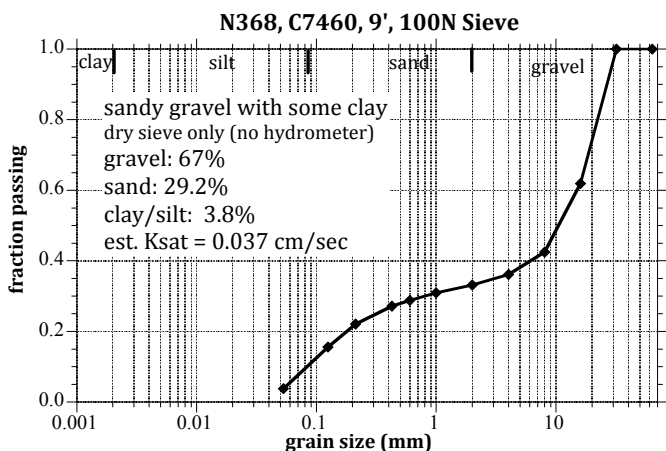


Appendix B

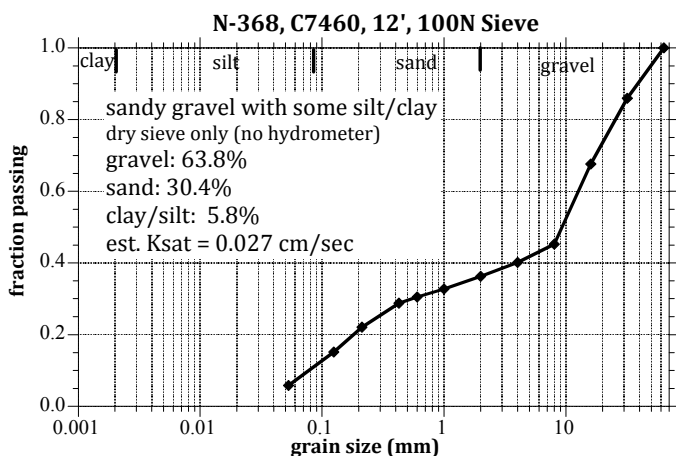
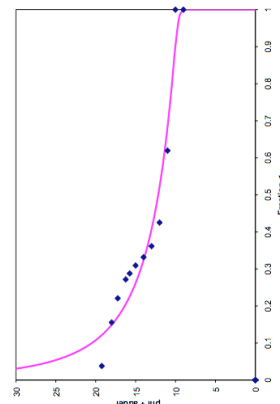
Well-Injection Grain-Size Distributions

Appendix B

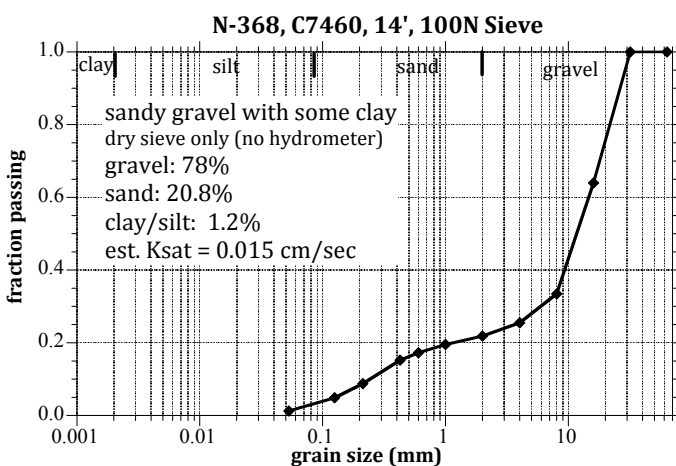
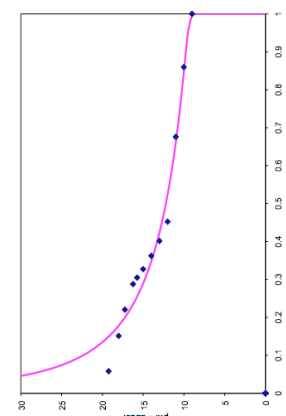
Well-Injection Grain-Size Distributions



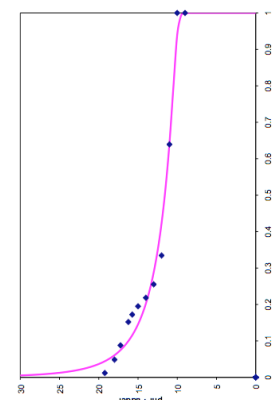
grain size (mm)	passing (fraction)
63.500	1.0000
31.750	1.0000
16.000	0.61947
8.0000	0.42533
4.0000	0.36154
2.0000	0.33172
1.0000	0.30932
0.60000	0.28785
0.42500	0.27175
0.21200	0.22077
0.12500	0.15554
0.053000	0.037980

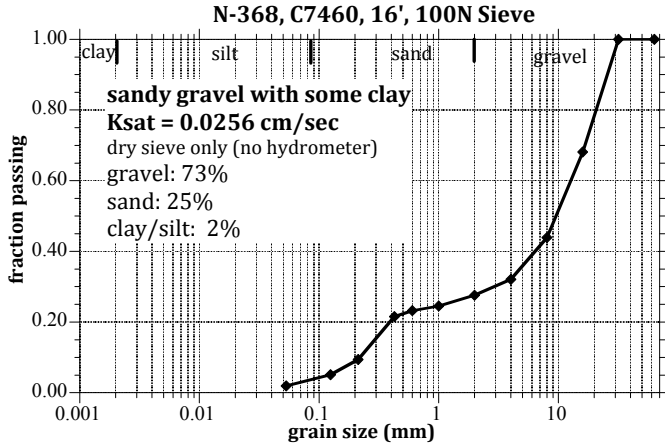


grain size (mm)	passing (fraction)
63.500	1.0000
31.750	0.85962
16.000	0.67603
8.0000	0.45230
4.0000	0.40144
2.0000	0.36234
1.0000	0.32736
0.60000	0.30501
0.42500	0.28781
0.21200	0.22064
0.12500	0.15126
0.053000	0.058210

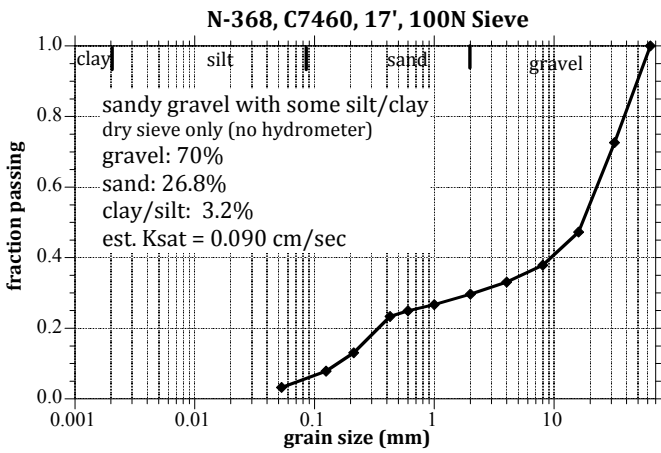
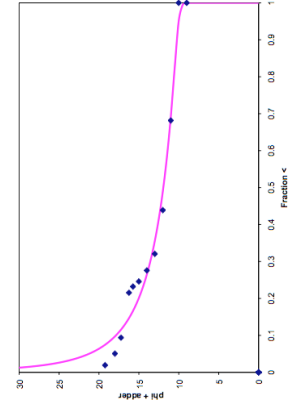


grain size (mm)	passing (fraction)
63.500	1.0000
31.750	1.0000
16.000	0.63937
8.0000	0.33454
4.0000	0.25530
2.0000	0.21839
1.0000	0.19516
0.60000	0.17236
0.42500	0.15210
0.21200	0.087930
0.12500	0.048580
0.053000	0.011990

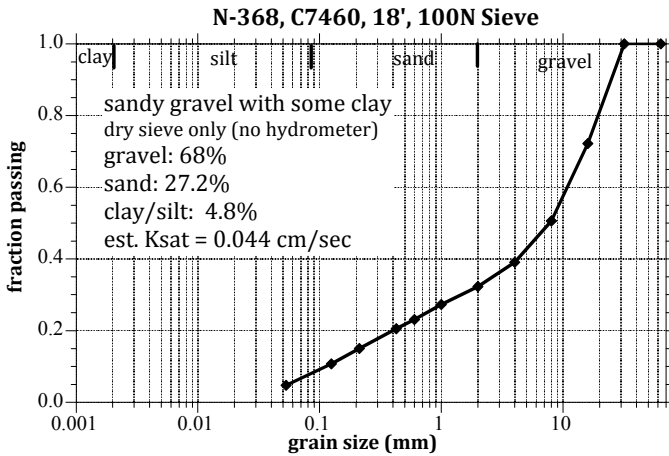
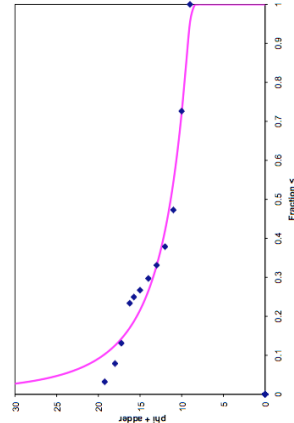




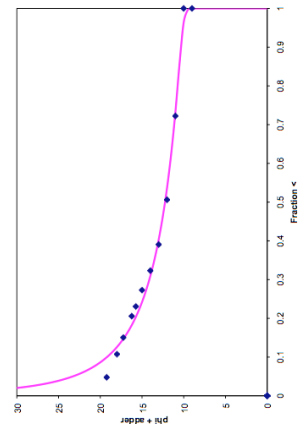
grain size (mm)	passing (fraction)
63.500	1.0000
31.750	1.0000
16.000	0.68162
8.0000	0.43897
4.0000	0.32069
2.0000	0.27584
1.0000	0.24590
0.60000	0.23214
0.42500	0.21555
0.21200	0.093910
0.12500	0.050740
0.053000	0.019330

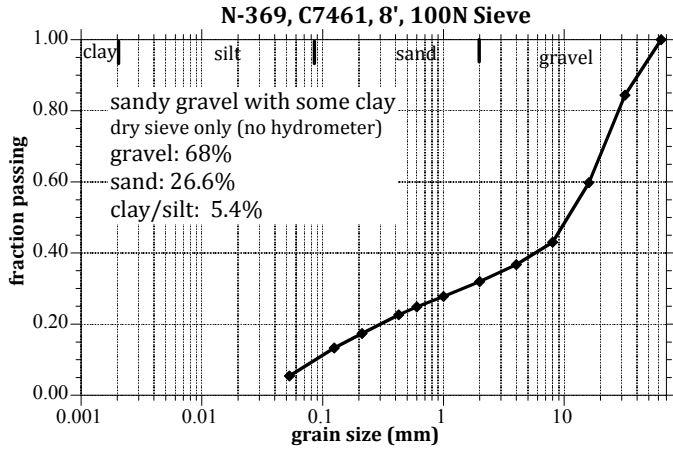


grain size (mm)	passing (fraction)
63.500	1.0000
31.750	0.72622
16.000	0.47277
8.0000	0.37866
4.0000	0.33107
2.0000	0.29707
1.0000	0.26717
0.60000	0.24948
0.42500	0.23355
0.21200	0.13107
0.12500	0.078940
0.053000	0.032170

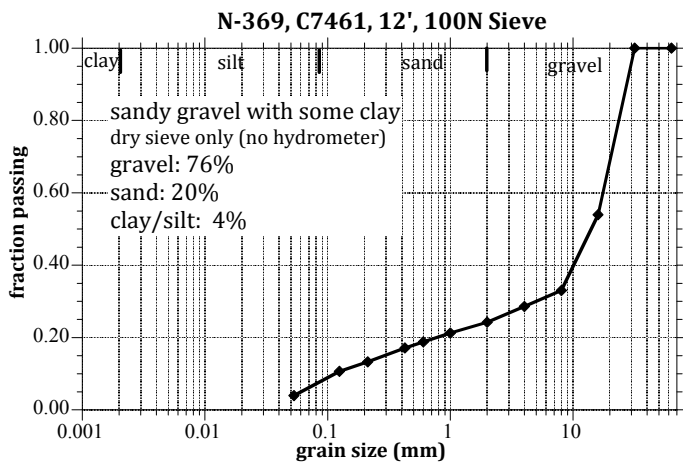
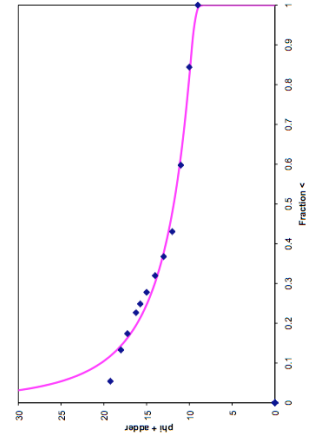


grain size (mm)	passing (fraction)
63.500	1.0000
31.750	1.0000
16.000	0.72240
8.0000	0.50618
4.0000	0.39066
2.0000	0.32304
1.0000	0.27284
0.60000	0.23069
0.42500	0.20568
0.21200	0.15044
0.12500	0.10747
0.053000	0.047730

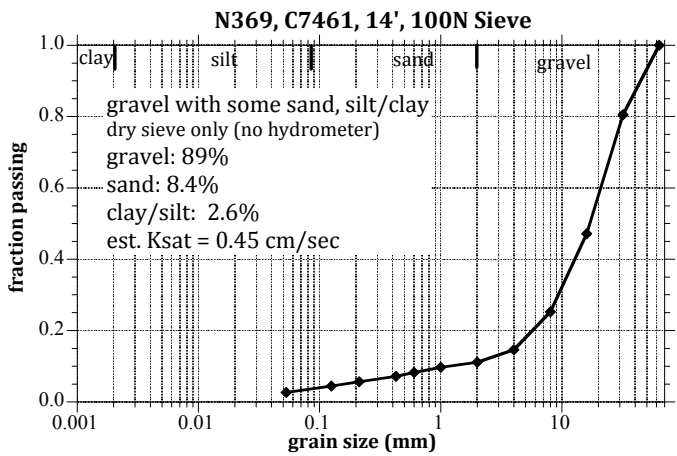
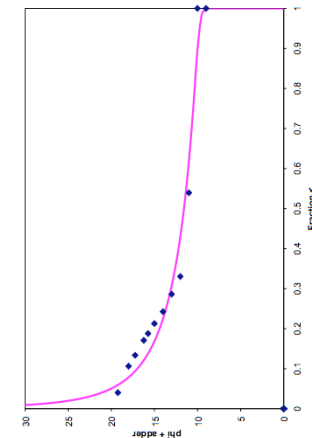




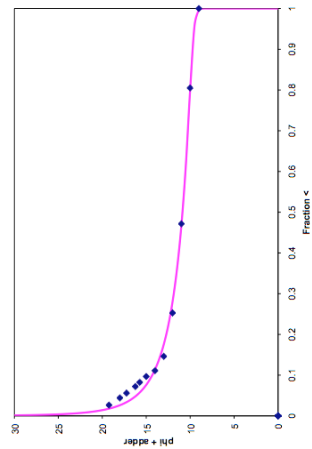
grain size (mm)	passing (fraction)
63.500	1.0000
31.750	0.84409
16.000	0.59763
8.0000	0.43049
4.0000	0.36764
2.0000	0.31980
1.0000	0.27794
0.60000	0.24866
0.42500	0.22673
0.21200	0.17396
0.12500	0.13293
0.053000	0.054240

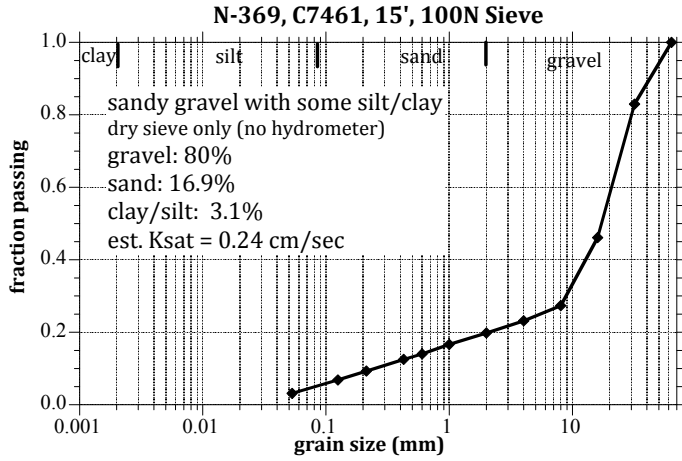


grain size (mm)	passing (fraction)
63.500	1.0000
31.750	1.0000
16.000	0.53949
8.0000	0.33035
4.0000	0.28613
2.0000	0.24243
1.0000	0.21278
0.60000	0.18781
0.42500	0.17085
0.21200	0.13349
0.12500	0.10623
0.053000	0.040160

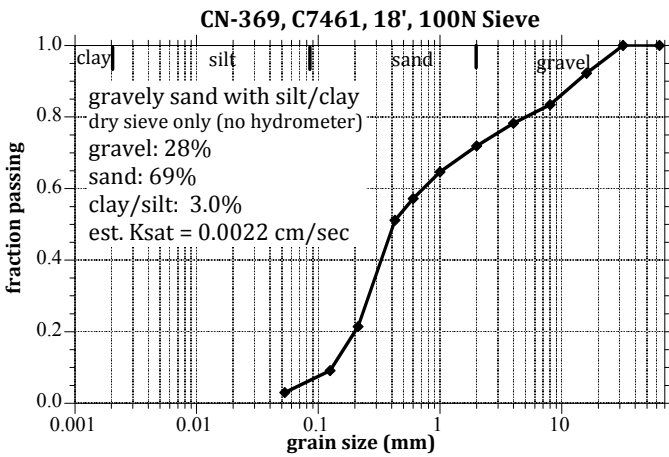
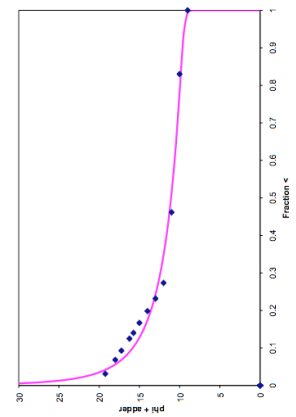


grain size (mm)	passing (fraction)
63.500	1.0000
31.750	0.80507
16.000	0.47163
8.0000	0.25285
4.0000	0.14617
2.0000	0.11104
1.0000	0.096770
0.60000	0.082510
0.42500	0.072070
0.21200	0.056000
0.12500	0.044180
0.053000	0.026510

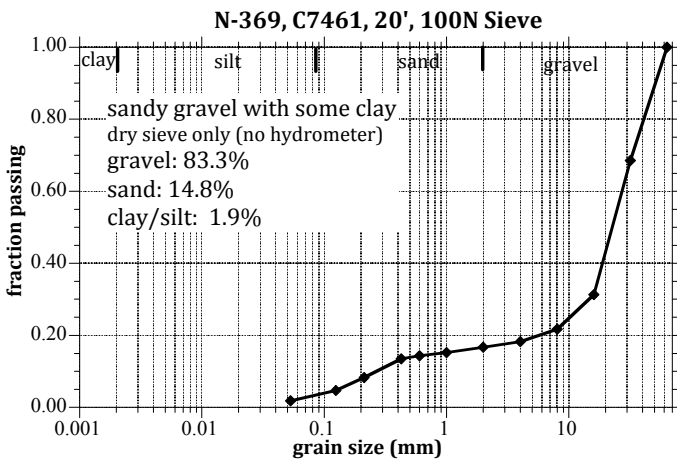
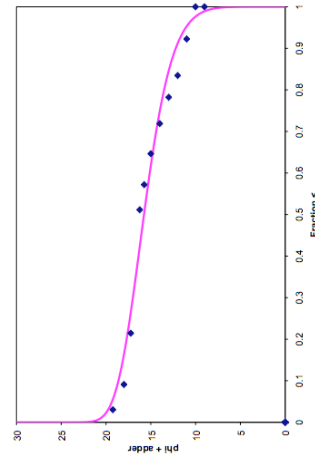




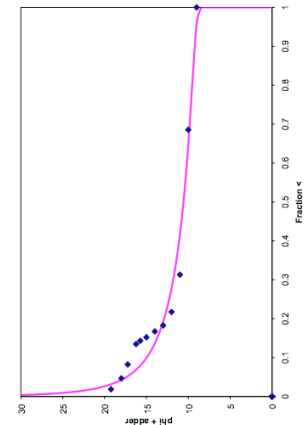
grain size (mm)	passing (fraction)
63.500	1.0000
31.750	0.83012
16.000	0.46158
8.0000	0.27345
4.0000	0.23169
2.0000	0.19841
1.0000	0.16692
0.60000	0.14020
0.42500	0.12490
0.21200	0.092910
0.12500	0.068360
0.053000	0.031230

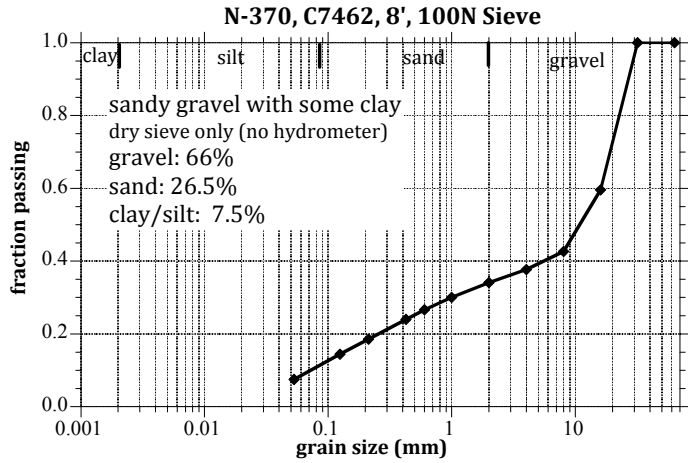


grain size (mm)	passing (fraction)
63.500	1.0000
31.750	1.0000
16.000	0.92257
8.0000	0.83467
4.0000	0.78232
2.0000	0.71902
1.0000	0.64646
0.60000	0.57195
0.42500	0.51157
0.21200	0.21451
0.12500	0.091060
0.053000	0.030440

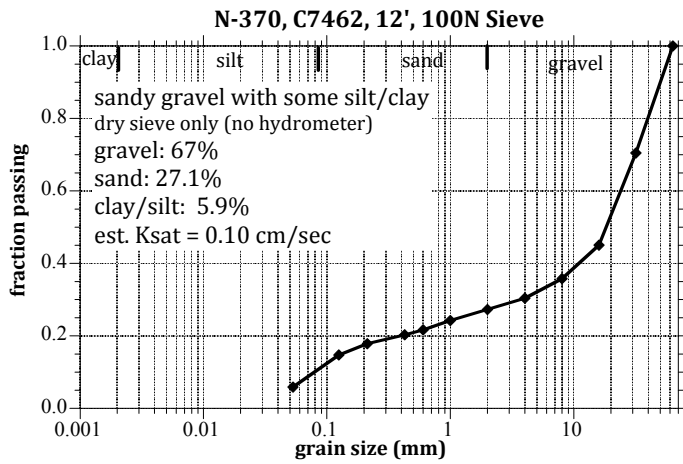
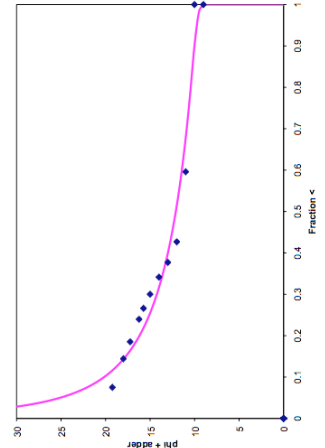


grain size (mm)	passing (fraction)
63.500	1.0000
31.750	0.68537
16.000	0.31297
8.0000	0.21732
4.0000	0.18268
2.0000	0.16722
1.0000	0.15218
0.60000	0.14326
0.42500	0.13485
0.21200	0.082370
0.12500	0.046680
0.053000	0.018570

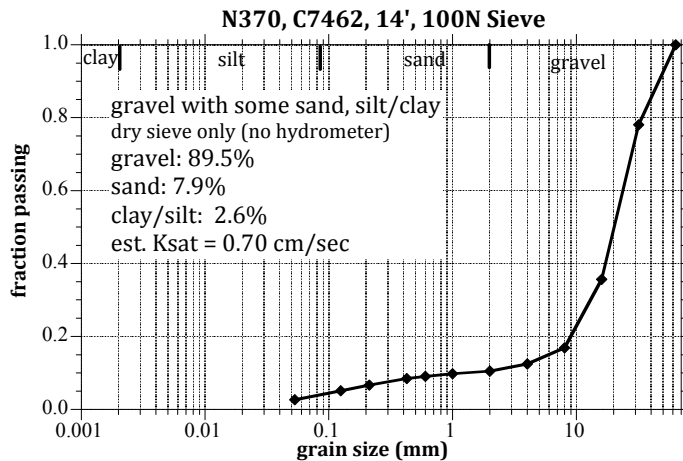
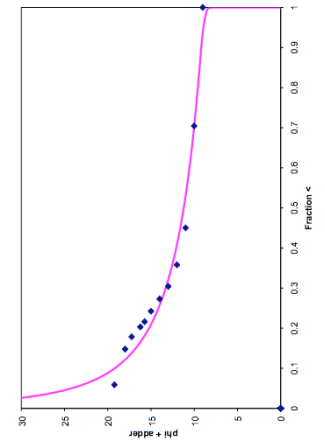




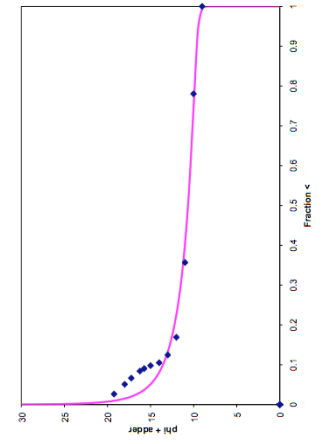
grain size (mm)	passing (fraction)
63.500	1.0000
31.750	1.0000
16.000	0.59605
8.0000	0.42675
4.0000	0.37705
2.0000	0.34151
1.0000	0.30024
0.60000	0.26610
0.42500	0.23974
0.21200	0.18529
0.12500	0.14434
0.053000	0.075090

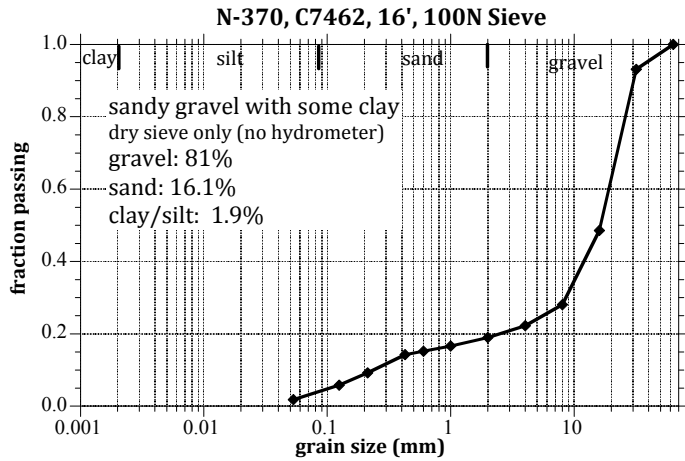


grain size (mm)	passing (fraction)
63.500	1.0000
31.750	0.70437
16.000	0.45026
8.0000	0.35814
4.0000	0.30425
2.0000	0.27307
1.0000	0.24236
0.60000	0.21636
0.42500	0.20320
0.21200	0.17860
0.12500	0.14774
0.053000	0.058910

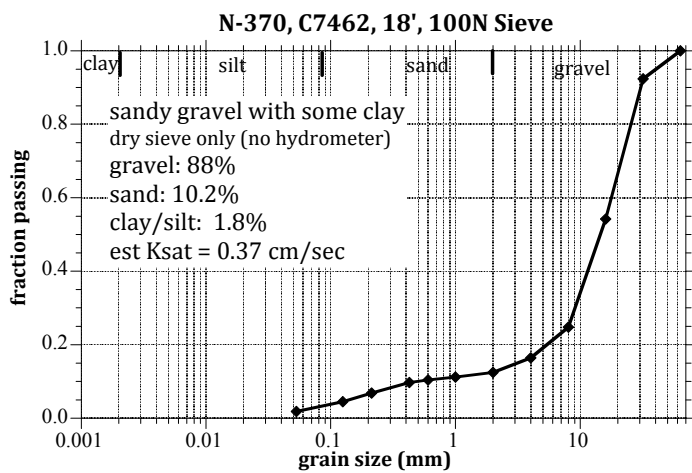
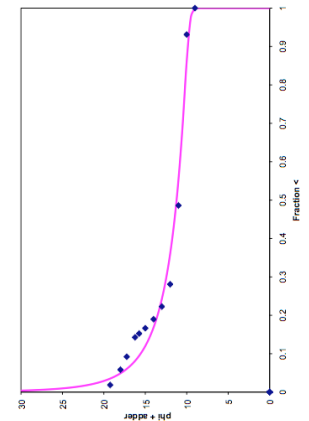


grain size (mm)	passing (fraction)
63.500	1.0000
31.750	0.78050
16.000	0.35682
8.0000	0.16915
4.0000	0.12478
2.0000	0.10507
1.0000	0.097910
0.60000	0.090650
0.42500	0.084280
0.21200	0.066670
0.12500	0.051040
0.053000	0.026570

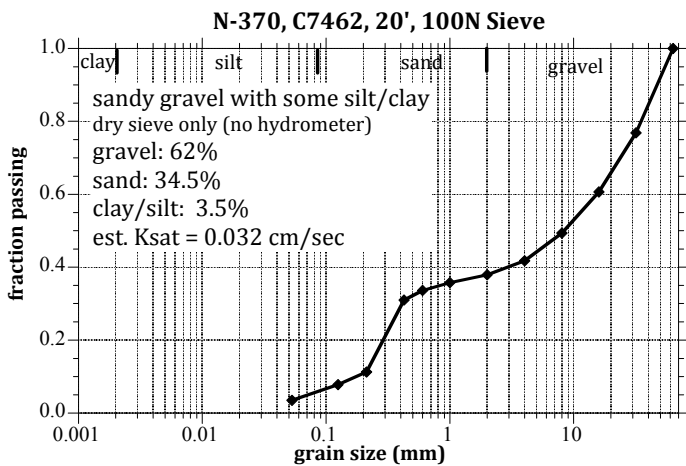
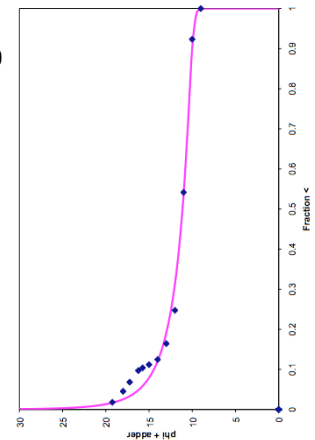




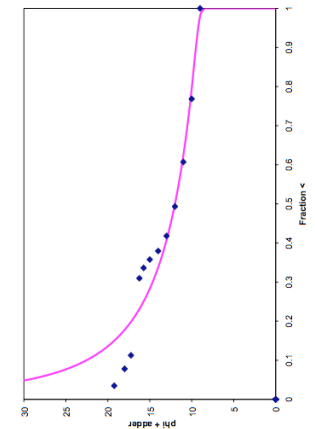
grain size (mm)	passing (fraction)
63.500	1.0000
31.750	0.93125
16.000	0.48606
8.0000	0.28086
4.0000	0.22280
2.0000	0.18979
1.0000	0.16642
0.60000	0.15248
0.42500	0.14274
0.21200	0.092120
0.12500	0.058370
0.053000	0.018550



grain size (mm)	passing (fraction)
63.500	1.0000
31.750	0.92347
16.000	0.54166
8.0000	0.24743
4.0000	0.16431
2.0000	0.12472
1.0000	0.11198
0.60000	0.10392
0.42500	0.097120
0.21200	0.068360
0.12500	0.045430
0.053000	0.018150



grain size (mm)	passing (fraction)
63.500	1.0000
31.750	0.76854
16.000	0.60716
8.0000	0.49340
4.0000	0.41798
2.0000	0.37949
1.0000	0.35758
0.60000	0.33624
0.42500	0.30969
0.21200	0.11264
0.12500	0.078090
0.053000	0.034830



Distribution

**No. of
Copies**

**No. of
Copies**

ONSITE

11 Pacific Northwest National Laboratory

**5 CH2M HILL Plateau Remediation
Company**

DJ Alexander	R3-60
NA Bowles (3)	R3-60
BP Esparza	R3-60

JS Fruchter	K6-96
N Qafoku	P7-58
ML Rockhold	K9-36
JE Szecsody (4)	K3-61
VR Vermeul	K6-96
MD Williams	K6-96
Hanford Technical Library (2)	P8-55



Pacific Northwest
NATIONAL LABORATORY

*Proudly Operated by **Battelle** Since 1965*

902 Battelle Boulevard
P.O. Box 999
Richland, WA 99352
1-888-375-PNNL (7665)

www.pnl.gov



U.S. DEPARTMENT OF
ENERGY